ASTRONOMY & ASTROPHYSICS
SUPPLEMENT SERIES

MAY II **2000**, PAGE 141

Astron. Astrophys. Suppl. Ser. **144**, 141–155 (2000)

Atomic data from the Iron Project⋆

XLIII. Transition probabilities for Fe V

S.N. Nahar[1], **F. Delahaye**[1], **A.K. Pradhan**[1], **and C.J. Zeippen**[2]

[1] Department of Astronomy, The Ohio State University, Columbus, OH 43210, U.S.A.
[2] UMR 8631, associée au CNRS et à l'Université Paris 7 et DAEC, Observatoire de Paris, F-92195 Meudon, France

Received December 23, 1999; accepted February 11, 2000

Abstract. An extensive set of dipole-allowed, intercombination, and forbidden transition probabilities for Fe V is presented. The Breit-Pauli R-matrix (BPRM) method is used to calculate 1.46 10^6 oscillator strengths for the allowed and intercombination E1 transitions among 3865 fine-structure levels dominated by configuration complexes with $n \leq 10$ and $l \leq 9$. These data are complemented by an atomic structure configuration interaction (CI) calculation using the SUPERSTRUCTURE program for 362 relativistic quadrupole (E2) and magnetic dipole (M1) transitions among 65 low-lying levels dominated by the $3d^4$ and $3d^3$ 4s configurations. Procedures have been developed for the identification of the large number of fine-structure levels and transitions obtained through the BPRM calculations. The target ion Fe VI is represented by an eigenfunction expansion of 19 fine-structure levels of $3d^3$ and a set of correlation configurations. Fe V bound levels are obtained with angular and spin symmetries $SL\pi$ and $J\pi$ of the (e + Fe VI) system such that $2S + 1 = 5$, 3, 1, $L \leq 10$, $J \leq 8$ of even and odd parities. The completeness of the calculated dataset is verified in terms of all possible bound levels belonging to relevant LS terms and transitions in correspondence with the LS terms. The fine-structure averaged relativistic values are compared with previous Opacity Project LS coupling data and other works. The 362 forbidden transition probabilities considerably extend the available data for the E2 and M1 transtions, and are in good agreement with those computed by Garstang for the $3d^4$ transitions.

Key words: atomic data

Send offprint requests to: S.N. Nahar

⋆ All data tables are available at the CDS via anonymous ftp (130.79.128.5) or http://cdsweb.u-strasbg.fr/Abstract.html

1. Introduction

Astrophysical and laboratory applications often require large datasets that are complete and accurate for comprehensive model calculations of opacities (Seaton et al. 1994, the Opacity Project Team 1995, 1996), radiative forces (e.g. Seaton 1997; Hui-Bon-Hoa & Alecian 1998; Seaton 1999), radiation transport in high-density fusion plasmas, etc. The Opacity Project (OP) (The Opacity Project 1995, 1996; Seaton et al. 1994) produced large datasets of transition probabilities for most astrophysically abundant atomic systems in the close coupling approximation using the powerful R-matrix method from atomic collision theory (Burke et al. 1971; Seaton 1987; Berrington et al. 1987). However, the calculations were carried out in LS coupling and the A-values were obtained neglecting relativistic fine-structure. The LS multiplets may be divided into fine-structure components using algebraic transformations. This has been done for a number of atoms and ions using the OP data (or similar non-relativistic calculations), including iron ions such as Fe II (Nahar 1995), Fe III (Nahar & Pradhan 1996), and Fe XIII (Nahar 1999). However, for such complex and heavy ions the neglect of relativistic effects may lead to a significant lack of precision, especially for weak transitions.

As an extension of the OP to include relativistic effects, the present Iron Project (IP) (Hummer et al. 1993) employs relativistic extensions of the R-matrix codes in the Breit-Pauli approximation (Scott & Burke 1980; Scott & Taylor 1982; Berrington et al. 1995) to compute radiative and collisional atomic parameters. Recently, several relativistic calculations of transition probabilities have been carried out using the Breit-Pauli R-matrix method (BPRM); e.g. for Fe XXV and Fe XXIV (Nahar & Pradhan 1999), C III (Berrington et al. 1998), Fe XXIII (Ramírez et al. 2000). These calculations produced highly accurate oscillator strengths for most transitions considered, within a few percent of experimental data or other accurate theoretical calculations (where available).

However, in these relatively simple atomic systems the electron correlation effects are weak and the configuration-interaction (CI, in the atomic structure sense) is easier to account for than in the more complex ions such as the low ionization stages of iron. In the present report we present the results of a large-scale BPRM calculation for one such ion, Fe V, and discuss the accuracy and completeness of the calculated data. An earlier work (Nahar & Pradhan 2000) has decribed certain important aspects of these calculations, in particular the difficulty with the identification of levels and completeness of fine-structure components within the LS multiplets. The general aim of the present work is two-fold: (i) to extend the IP work to the calculation of relativistic transition probabilities for the complex low-z iron ions, and (ii) to provide a detailed description of the extensive data tables that should be essentially complete for most applications.

2. Theory

The theoretical scheme is described in earlier works (Hummer et al. 1993; Nahar & Pradhan 1999, 2000). We sketch the basic points below. In the coupled channel or close coupling (CC) approximation an atom (ion) is described in terms of an (e + ion) complex that comprises of a "target" ion, with N bound electrons, and a "free" electron that may be either bound or continuum. The total energy of the system is either negative or positive; negative eigenvalues of the $(N + 1)$-electron Hamiltonian correspond to bound states of the (e + ion) system. In the CC approximation the wavefunction expansion, $\Psi(E)$, for a total spin and angular symmetry $SL\pi$ or $J\pi$, of the $(N+1)$ electron system is represented in terms of the target ion states or levels as:

$$\Psi_{\rm E}({\rm e + ion}) = A\sum_i \chi_i({\rm ion})\theta_i + \sum_j c_j\Phi_j, \qquad (1)$$

where χ_i is the target ion wave function in a specific state $S_iL_i\pi_i$ or level $J_i\pi_i$, and θ_i is the wave function for the $(N+1)$th electron in a channel labeled as $S_iL_i(J_i)\pi_i\ \ k_i^2\ell_i(SL\pi)\ \ [J\pi]$; k_i^2 is the incident kinetic energy. In the second sum the Φ_j's are correlation wavefunctions of the $(N+1)$ electron system that (a) compensate for the orthogonality conditions between the continuum and the bound orbitals, and (b) represent additional short-range correlation that is often of crucial importance in scattering and radiative CC calculations for each $SL\pi$.

The BPRM method yields the solutions of the relativistic CC equations using the Breit-Pauli Hamiltonian for the $(N+1)$-electron system to obtain the total wavefunctions $\Psi_{\rm E}({\rm e + ion})$ (Hummer et al. 1993). The BP Hamiltonian is

$$H^{\rm BP}_{N+1} = H_{N+1} + H^{\rm mass}_{N+1} + H^{\rm Dar}_{N+1} + H^{\rm so}_{N+1}, \qquad (2)$$

where H_{N+1} is the nonrelativistic Hamiltonian,

$$H_{N+1} = \sum_{i=1}^{N+1}\left\{-\nabla_i^2 - \frac{2Z}{r_i} + \sum_{j>i}^{N+1}\frac{2}{r_{ij}}\right\}, \qquad (3)$$

and the additional terms are the one-body terms, the mass correction, the Darwin and the spin-orbit terms respectively. The spin-orbit interaction splits the LS terms into fine-structure levels $J\pi$, where J is the total angular momentum. The positive and negative energy states (Eq. 1) define continuum or bound (e + ion) states,

$$\begin{aligned} &E = k^2 > 0 \longrightarrow \text{continuum (scattering) channel} \\ &E = -\tfrac{z^2}{\nu^2} < 0 \longrightarrow \text{bound state,} \end{aligned} \qquad (4)$$

where ν is the effective quantum number relative to the core level. Determination of the quantum defect $(\mu(\ell))$, defined as $\nu_i = n - \mu(\ell)$ where ν_i is relative to the core level $S_iL_i\pi_i$, is helpful in establishing the ℓ-value associated with a given channel level.

The $\Psi_{\rm E}$ represents a CI-type wavefunction over a large number of electronic configurations depending on the target levels included in the eigenfunction expansion (Eq. 1). Transition matrix elements may be calculated with these wavefunctions, and the electron dipole (E1), electric quadrupole (E2), magnetic dipole (M1) or other operators to obtain the corresponding transition probabilities. The present version of the BPRM codes implements the E1 operator to enable the calculation of dipole allowed and intercombination transition probabilities. The oscillator strength is proportional to the generalized line strength defined, in either length form or velocity form, by the equations

$$S_{\rm L} = \left|\left\langle \Psi_{\rm f}\right| \sum_{j=1}^{N+1} r_j \left|\Psi_{\rm i}\right\rangle\right|^2 \qquad (5)$$

and

$$S_{\rm V} = \omega^{-2}\left|\left\langle \Psi_{\rm f}\right| \sum_{j=1}^{N+1} \frac{\partial}{\partial r_j} \left|\Psi_{\rm i}\right\rangle\right|^2. \qquad (6)$$

In these equations ω is the incident photon energy in Rydberg units, and $\Psi_{\rm i}$ and $\Psi_{\rm f}$ are the bound wave functions representing the initial and final states respectively. The line strengths are energy independent quantities.

Using the energy difference, E_{ji}, between the initial and final states, the oscillator strength, f_{ij}, for the transition can be obtained from S as

$$f_{ij} = \frac{E_{ji}}{3g_i}S, \qquad (7)$$

and the Einstein's A-coefficient, A_{ji}, as

$$A_{ji}({\rm a.u.}) = \frac{1}{2}\alpha^3\frac{g_i}{g_j}E_{ji}^2 f_{ij}, \qquad (8)$$

where α is the fine structure constant, and g_i, g_j are the statistical weight factors of the initial and final states, respectively. In cgs units,

$$A_{ji}({\rm s}^{-1}) = \frac{A_{ji}({\rm a.u.})}{\tau_0}, \qquad (9)$$

where $\tau_0 = 2.4191\ 10^{-17}$ s is the atomic unit of time.

3. Computations

3.1. The BPRM calculations

The Fe V wavefunctions are computed with eigenfunction expansions over the "target" ion Fe VI. Present work employs a 19-level eigenfunction expansion of Fe VI corresponding to the 8-term LS basis set of $3d^3(^4F$, ^4P, ^2G, ^2P, $^2D2$, ^2H, ^2F, $^2D1)$, as used in Nahar & Pradhan (2000). The target wavefunctions were obtained by Chen & Pradhan (1999) using the Breit-Pauli version of the atomic structure code, SUPERSTRUCTURE (Eissner et al. 1974). The bound channel set of functions Φ_j in Eq. (1), representing additional $(N+1)$-electron correlation includes a number of Fe V configurations, particularly from the important $n = 3$ complex, i.e. $3s^23p^63d^4$, $3p^63d^6$, $3s^23p^53d^5$, $3s^23p^43d^6$; the complete list of Φ_j for the $n = 3$ and 4 configurations is given in Chen & Pradhan (1999).

The Breit-Pauli calculations consider all possible fine-structure bound levels of Fe V with $(2S + 1) = 1$, 3, 5 and $L = 0 - 10$, $n \leq 10$, $\ell \leq n - 1$, and $J \leq 8$, and the transitions among these levels. In the R-matrix computations, the calculated energies of the target levels were replaced by the observed ones. The calculations are carried out using the BPRM codes (Berrington et al. 1995) extended from the Opacity Project codes (Berrington et al. 1987).

STG1 of the BPRM codes computes the one- and two-electron radial integrals using the one-electron target orbitals generated by SUPERSTRUCTURE. The number of continuum R-matrix basis functions is chosen to be 12. The intermediate coupling calculations are carried out on recoupling these LS symmetries in a pair-coupling representation in stage RECUPD. The computer memory requirement for this stage has been the maximum as it carries out angular algebra of dipole matrix elements of a large number of levels due to fine-structure splitting. The (e + Fe VI) Hamiltonian is diagonalized for each resulting $J\pi$ in STGH.

3.1.1. Energy levels and identification

The negative eigenvalues of the (e + Fe VI) Hamiltonian correspond to the bound levels of Fe V, determined using the code STGB. Splitting of each target LS term into its fine-structure components also increases the number of Rydberg series of levels converging on to them. These result in a large number of fine-structure levels in comparatively narrow energy bands. An order of magnitude finer mesh of effective quantum number ($\Delta\nu = 0.001$), compared to that needed for the locating the bound LS states, was needed to search for the BP Hamitonian eigenvalues in order to avoid missing energy levels. The computational requirements were, therefore, increased considerably for the intermediate coupling calculations of bound levels over the LS coupling case by several orders of magnitude. The calculations take up to several CPU hours per $J\pi$ in order to determine the corresponding eigenvalues in the asymptotic program STGB.

The identification of the fine-structure bound levels computed in intermediate coupling using the collision theory BPRM method is rather involved, since they are labeled with quantum numbers related to electron-ion scattering channels. The levels are associated with collision complexes of the (e + ion) system which, in turn, are initially identified only with their total angular momenta and parity, $J\pi$. A scheme has been developed (Nahar & Pradhan 2000) to identify the levels with complete spectroscopic information giving

$$C_{\rm t}(\ S_{\rm t}\ L_{\rm t})\ J_{\rm t}\ \pi_{\rm t} n\ell\ [{\rm K}]{\rm s}\ \ J\ \pi, \qquad (10)$$

and also to designate the levels with a possible $SL\pi$ symmetry ($C_{\rm t}$ is the target configuration).

Most of the spectroscopic information of a computed level is extracted from the few bound channels that dominate the wavefunction of that level. A new code PRCBPID has been developed to carry out the identification, including quantum defect analysis and angular momentum algebra of the dominant channels. Two additional problems are addressed in the identification work: (A) correspondence of the computed fine-structure levels to the standard LS coupling designation, $SL\pi$, and (B) completeness checks for the set of all fine-structure components within all computed LS multiplets. A correspondence between the sets of $SL\pi$ and $J\pi$ of the same configuration are established from the set of $SL\pi$ symmetries, formed from the target term, $S_{\rm t}L_{\rm t}\pi_{\rm t}$, nl quantum numbers of the valence electron, and $J\pi$ of the fine-structure level belonging to the LS term. The identification procedure is described in detail in Nahar & Pradhan (2000).

Considerable effort has been devoted to a precise and unique identification of levels. However, a complex ion such as Fe V involves many highly mixed levels and it becomes difficult to assign a definite configuration and parentage to all bound states. Nonetheless, most of the levels have been uniquely identified. In particular all calculated levels corresponding to the experimentally observed ones are correctly (and independently) assigned to their proper spectroscopic designation by the identification procedure employed.

3.1.2. E1 oscillator strengths

The oscillator strengths and transition probabilities were obtained using STGBB of the BPRM codes. STGBB computed the transition matrix elements using the bound wavefunctions created by STGB, and the dipole operators computed by STGH. The fine structure of the core and the $(N+1)$ electron system increased the computer memory and CPU time requirements considerably over the LS coupling calculations. About 31 MW of memory, and about one CPU hour on the Cray T94, was required

to compute the oscillator strengths for transitions among the levels of a pair of $J\pi$ symmetries. These are over an order of magnitude larger than those needed for f-values in LS coupling. The number of f-values obtained from the BPRM calculations ranges from over 5000, among $J = 8$ levels, to over 123000, among $J = 3$ levels, for a pair of symmetries.

These computations required over 120 CPU hours on the Cray T94. Total memory size needed was over 42 MW to diagonalise the BP Hamilitonian. Largest computations involved a single $J\pi$ Hamiltonian of matrix size 3555, 120 channels, and 2010 configurations.

We have included extensive tables of all computed bound levels, and associated E1 A-values, with full spectroscopic identifications, as standardized by the U.S. National Institute for Standards and Technology (NIST). In addition, rather elaborate (though rather tedious) procedures are implemented to check and ensure completeness of fine-structure components within all computed LS multiplets. The complete data tables are available in electronic format. A sample of the datasets is described in the next section.

3.2. SUPERSTRUCTURE calculations for the forbidden E2, M1 transitions

The only available dataset by Garstang (1957) comprises of the E2, M1 A-values for transitions within the ground $3d^4$ levels. The CI expansion for Fe V consists of the configurations ($1s^22s^22p^63s^23p^6$) $3d^4$, $3d^34s$, $3d^34p$ as the spectroscopic configurations and $3d^34d$, $3d^35s$, $3d^35p$, $3d^35d$, $3d^24s^2$, $3d^24p^2$, $3d^24d^2$, $3d^24s4p$, $3d^24s4d$ as correlation configurations. The eigenenergies of levels dominated by the spectroscopic configurations are minimised with scaling parameters $\lambda_{n\ell}$ in the Thomas-Fermi-Dirac potential used to calculate the one-electron orbitals in SUPERSTRUCTURE (see Nussbaumer & Storey 1978): $\lambda_{[1s-5d]} = 1.42912$, 1.13633, 1.08043, 1.09387, 1.07756, 0.99000, 1.09616, 1.08171, −0.5800, −0.6944, −1.0712, −3.0000.

There are 182 fine-structure levels dominated by the configurations $3d^4$, $3d^34s$ and $3d^34p$, and the respective number of LS terms is 16, 32 and 80. The λ_{1s-3d} are minimised over the first 16 terms of $3d^4$, λ_{4s} over 32 terms including $3d^34s$, and λ_{4p}, λ_{5p} over all 80 terms. The λ_{5s} and λ_{5d} are optimised over the $3d^4$ terms to further improve the corresponding eigenfunctions.

The numerical experimentation entailed a number of minimisation trials, with the goal of optimisation over most levels. The final set of calculated energies agree with experiment to within 10%, although more selective optimisation can lead to much better agreement for many (but not all) levels. Finally, semi-empirical term energy corrections (TEC) (Zeippen et al. 1977) were applied to obtain the transition probabilities. This procedure has been successfully applied in a large number of studies (see e.g. Biémont et al. 1994). The electric quadrupole (E2) and the magnetic dipole (M1) transition probabilites, $A^{\rm q}$ and $A^{\rm m}$, are obtained using observed energies according to the expressions:

$$A^{\rm q}_{j,i}({\rm E2}) = 2.6733\ 10^3(E_j - E_i)^5\mathcal{S}^{\rm q}(i,j){\rm s}^{-1}, \quad (11)$$

and

$$A^{\rm m}_{j,i}({\rm M1}) = 3.5644\ 10^4(E_j - E_i)^3\mathcal{S}^{\rm m}(i,j){\rm s}^{-1}, \quad (12)$$

where $E_j > E_i$ (the energies are in Rydbergs), and $\mathcal{S}$ is the line strength for the corresponding transition.

4. Results and discussion

We have obtained nearly 1.5 10^6 oscillator strengths for bound-bound transitions in Fe V. To our knowledge there are no previous ab initio relativistic calculations for transition probabilities for Fe V. The previous Opacity Project data consists of approximately 30000 LS transitions. Therefore the new dataset of nearly 1.5 10^6 oscillator strengths should significantly enhance the database, and the range and precision of related applications, some of which we discuss later.

We divide the discussion of energies and oscillator strengths in the subsections below.

4.1. Fine-structure levels from the BPRM calculations

A total of 3 865 fine-structure bound levels of Fe V have been obtained for $J\pi$ symmetries, $0 \le J \le 8$ even and odd parities. These belong to symmetries $2S + 1 = 5$, 3, 1, $0 \le L \le 9$, with $n \le 10$ and $0 \le l \le 9$. The BPRM calculations initially yield only the energies and the total symmetry, $J\pi$, of the levels. Through an identification procedure based on the analysis of quantum defects and percentage channel contributions for each level in the region outside the R-matrix boundary (described in Nahar & Pradhan 2000), the levels are assigned with possible designation of $C_{\rm t}(S_{\rm t}L_{\rm t})J_{\rm t}\pi_{\rm t}nlJ(SL)\pi$, which specifies the core or target configuration, LS term and parity, and total angular momentum; the principal and orbital angular momenta, nl, of the outer or the valence electron; the total angular momentum, J, and the possible LS term and parity, $SL\pi$, of the $(N+1)$-electron bound level. Table 1a presents a few partial sets of energy levels from the complete set available electronically.

4.1.1. Computed order of levels according to $J\pi$

Examples of fine structure energy levels are presented in sets of $J\pi$ in Table 1a where their assigned identifications are given. N_J is the total number of energy levels for the

symmetry $J\pi$ (e.g. there are 80 levels with $J\pi = 0^e$, although the table presents only 25 of them). The effective quantum number, $\nu = z/\sqrt{(E - E_t)}$ where E_t is the energy of the target state, is also given for each level. The ν is not given for any equivalent electron level as it is undefined. In the core configuration, the first digit after each orbital specifies the occupancy number. The second digit, in some cases, refers to the seniority of the core term (e.g. in "3d32", "3d3" refers to the core configuration and "2" refers to the seniority number of the associated core term). An unidentifiable level is often assigned with a possible equivalent electron level. In Table 1a, one level of $J\pi = 0^\circ$ is assigned to the equivalent electron configuration, $3p^5 3d^5$. The assignment is based on two factors: (a) the calculated ν of the level does not match with that of any valence electon, and (b) the wavefunction is represented by a number of channels of similar percentage weights, i.e., no dominant channel. The configuration $3p^5 3d^3$ corresponds to a large number of LS terms. However, the level can not be identified with any particular term through quantum defect analysis. Hence it is designated as ^0S, indicating an undetermined spectroscopic term.

4.1.2. Energy order of levels

In Table 1b a limited selection of energy levels is presented in a format different from that in Table 1a. Here they are listed in ascending energy order regardless of $J\pi$ values, and are grouped together within the same configuration to show the correspondence between the sets of J-levels and the LS terms. This format provides a check of completeness of sets of energy levels in terms of LS terms, and also determines the missing levels. Levels grouped in such a manner also show closely spaced energies, consistent with the fact that they are fine-structure components with a given LS term designation. The title of each set in Table 1b lists all possible LS terms that can be formed from the core or target term, and outer or the valence electron angular momentum. "Nlv" is the total number of J-levels that correspond to the set of LS terms. The spin multiplicity $(2S + 1)$ and parity (π) are given next. The J values for each term is given within parentheses next to the corresponding L. At the end of the set of levels, "Nlv(c)" is the total number of J-levels obtained in the calculations. Hence, if Nlv = Nlv(c) for a set of levels of the same configuration the set is designated as "complete".

Most sets of fine-structure components between LS multiplets are found to be complete. High lying energy levels often belong to incomplete sets. The possible LS terms for each level is specified in the last column. It is seen that a level may possibly belong to several LS terms. In the absence any other criteriion, the proper term for the level may be assumed by applying Hund's rule: with levels of the same spin multiplicity, the highest L-level is

Table 1. a). Identified fine-strucuture energy levels of Fe V. N_J = total number of levels for the symmetry $J\pi$

i	C_t	$S_tL_t\pi_t$	J_t	nl	J	$E_c(Ry)$	ν	$SL\pi$
			N_J= 80,			$J\pi$= 0^e		
1	3d4				0	−5.56210E+00		^{5} De
2	3d4				0	−5.34705E+00		^{3} Pe
3	3d4				0	−5.16997E+00		^{1} Se
4	3d4				0	−4.96162E+00		^{3} Pe
5	3d4				0	−4.43020E+00		^{1} Se
6	3d3	^{4}P^e	1/2	4s	0	−3.47060E+00	2.62	^{3} Pe
7	3d3	^{2}P^e	1/2	4s	0	−3.44860E+00	2.60	^{3} Pe
8	3d3	^{4}F^e	3/2	4d	0	−2.28673E+00	3.31	^{5} De
9	3d3	^{4}F^e	5/2	4d	0	−2.24585E+00	3.33	^{3} Pe
10	3d3	^{4}P^e	3/2	4d	0	−2.08337E+00	3.33	^{5} De
11	3d3	^{4}P^e	5/2	4d	0	−2.07641E+00	3.33	^{3} Pe
12	3d32	^{2}D^e	3/2	4d	0	−2.03154E+00	3.30	^{3} Pe
13	3d3	^{2}P^e	3/2	4d	0	−1.94013E+00	3.39	^{3} Pe
14	3d32	^{2}D^e	5/2	4d	0	−1.84426E+00	3.45	^{1} Se
15	3d3	^{4}P^e	1/2	5s	0	−1.76456E+00	3.59	^{3} Pe
16	3d3	^{2}F^e	5/2	4d	0	−1.73641E+00	3.40	^{3} Pe
17	3d3	^{2}P^e	1/2	5s	0	−1.70995E+00	3.58	^{3} Pe
18	3d31	^{2}D^e	3/2	4d	0	−1.54486E+00	3.37	^{1} Se
19	3d31	^{2}D^e	5/2	4d	0	−1.32130E+00	3.56	^{3} Pe
20	3d3	^{4}F^e	3/2	5d	0	−1.27240E+00	4.43	^{5} De
21	3d3	^{4}F^e	5/2	5d	0	−1.25685E+00	4.45	^{3} Pe
22	3d3	^{4}P^e	3/2	5d	0	−1.11887E+00	4.40	^{5} De
23	3d3	^{4}P^e	5/2	5d	0	−1.08686E+00	4.44	^{3} Pe
24	3d3	^{2}P^e	3/2	5d	0	−1.03290E+00	4.43	^{3} Pe
25	3d32	^{2}D^e	3/2	5d	0	−1.02130E+00	4.42	^{3} Pe
			N_J= 85,			$J\pi$ = 0°		
1	3d3	^{4}F^e	3/2	4p	0	−3.14690E+00	2.82	^{5} D°
2	3d3	^{4}P^e	1/2	4p	0	−2.97968E+00	2.82	^{5} D°
3	3d3	^{4}P^e	3/2	4p	0	−2.96755E+00	2.82	^{3} P°
4	3d3	^{2}P^e	1/2	4p	0	−2.94580E+00	2.80	^{1} S°
5	3d3	^{2}P^e	3/2	4p	0	−2.93098E+00	2.81	^{3} P°
6	3d32	^{2}D^e	3/2	4p	0	−2.82995E+00	2.84	^{3} P°
7	3d31	^{2}D^e	3/2	4p	0	−2.41156E+00	2.85	^{3} P°
8	3d3	^{4}F^e	3/2	5p	0	−1.68614E+00	3.85	^{5} D°
9	3d3	^{4}F^e	5/2	4f	0	−1.59067E+00	3.96	^{3} P°
10	3d3	^{4}F^e	7/2	4f	0	−1.58408E+00	3.96	^{5} D°
11	3d3	^{4}P^e	1/2	5p	0	−1.51986E+00	3.84	^{5} D°
12	3d3	^{4}P^e	3/2	5p	0	−1.51338E+00	3.85	^{3} P°
13	3d3	^{2}P^e	3/2	5	0	−1.45761E+00	3.84	^{3} P°
14	3d3	^{2}P^e	1/2	5p	0	−1.45430E+00	3.84	^{1} S°
15	3d32	^{2}D^e	3/2	5p	0	−1.41826E+00	3.86	^{3} P°
16	3d3	^{4}P^e	5/2	4f	0	−1.40953E+00	3.97	^{5} D°
17	3d3	^{2}G^e	7/2	4f	0	−1.39869E+00	3.97	^{3} P°
18	3d32	^{2}D^e	5/2	4f	0	−1.34962E+00	3.94	^{3} P°
19	3d3	^{2}F^e	7/2	4f	0	−1.17207E+00	3.96	^{3} P°
20	3d3	^{2}F^e	5/2	4f	0	−1.16069E+00	3.97	^{1} S°
21	3p53d5				0	−1.10428E+00		^{0} S°
22	3d3	^{4}F^e	3/2	6p	0	−1.05635E+00	4.86	^{5} D°
23	3d3	^{4}F^e	5/2	5f	0	−1.01782E+00	4.94	^{5} D°
24	3d3 1	^{2}D^e	3/2	5p	0	−1.01063E+00	3.87	^{3} P°
25	3d3	^{4}F^e	7/2	5f	0	−1.00821E+00	4.95	^{3} P°
			N_J= 236,			$J\pi$ = 1°		
1	3d3	^{4}F^e	3/2	4p	1	−3.14950E+00	2.82	^{5} DF°
2	3d3	^{4}F^e	3/2	4p	1	−3.14082E+00	2.82	^{5} DF°
3	3d3	^{4}F^e	5/2	4p	1	−3.13088E+00	2.82	^{3} D°
4	3d3	^{4}P^e	3/2	4p	1	−2.99367E+00	2.81	^{5} PD°
5	3d3	^{4}P^e	1/2	4p	1	−2.97465E+00	2.82	^{5} PD°
6	3d3	^{4}P^e	3/2	4p	1	−2.96345E+00	2.82	^{3} SPD°
7	3d3	^{2}P^e	1/2	4p	1	−2.93263E+00	2.81	^{3} SPD°
8	3d32	^{2}D^e	5/2	4p	1	−2.90308E+00	2.82	^{1} P°
9	3d32	^{2}D^e	5/2	4p	1	−2.88417E+00	2.82	^{3} PD°
10	3d3	^{2}P^e	1/2	4p	1	−2.87902E+00	2.83	^{3} SPD°
11	3d3	^{2}P^e	3/2	4p	1	−2.86205E+00	2.84	^{3} SPD°
12	3d3	^{4}P^e	1/2	4p	1	−2.84777E+00	2.88	^{3} SPD°
13	3d32	^{2}D^e	3/2	4p	1	−2.83128E+00	2.84	^{3} PD°
14	3d3	^{2}P^e	3/2	4p	1	−2.78217E+00	2.88	^{1} P°
15	3d3	^{4}P^e	5/2	4p	1	−2.77047E+00	2.91	^{3} SPD°
16	3d3	^{2}F^e	5/2	4p	1	−2.65585E+00	2.85	^{3} D°
17	3d31	^{2}D^e	3/2	4p	1	−2.49355E+00	2.82	^{3} PD°
18	3d31	^{2}D^e	3/2	4p	1	−2.41413E+00	2.85	^{3} PD°
19	3d31	^{2}D^e	5/2	4p	1	−2.33944E+00	2.89	^{1} P°
20	3d3	^{4}F^e	3/2	5p	1	−1.68531E+00	3.85	^{5} DF°

Table 1. b). Ordered and identified fine-structure energy levels of Fe V. Nlv = total number of levels expected for the possible LS terms listed, and Nlv(c) = number of levels calculated. $SL\pi$ lists the possible LS terms for each level (see text for details)

C_t	$S_tL_t\pi_t$	J_t	nl	J	E(cal)	ν	$SL\pi$
Nlv = 5, 5,e:	F (5 4 3 2 1)						
3d3	(4Fe)	3/2	4s	1	−3.73515E+00	2.59	5 F e
3d3	(4Fe)	5/2	4s	2	−3.73238E+00	2.59	5 F e
3d3	(4Fe)	5/2	4s	3	−3.72820E+00	2.59	5 F e
3d3	(4Fe)	7/2	4s	4	−3.72275E+00	2.59	5 F e
3d3	(4Fe)	9/2	4s	5	−3.71610E+00	2.59	5 F e
Ncal = 5: set complete							
Nlv = 3, 3,e:	F (4 3 2)						
3d3	(4Fe)	3/2	4s	2	−3.63808E+00	2.62	3 F e
3d3	(4Fe)	7/2	4s	3	−3.63107E+00	2.62	3 F e
3d3	(4Fe)	9/2	4s	4	−3.62225E+00	2.62	3 F e
Ncal = 3: set complete							
Nlv = 3, 1,o:	P (1) D (2) F (3)						
3d3 1	(2De)	3/2	4p	2	−2.45812E+00	2.83	1 D o
3d3 1	(2De)	5/2	4p	3	−2.40581E+00	2.86	1 F o
3d3 1	(2De)	5/2	4p	1	−2.33944E+00	2.89	1 P o
Ncal = 3: set complete							
Nlv = 23, 5,e:	P (3 2 1) D (4 3 2 1 0) F (5 4 3 2 1) G (6 5 4 3 2) H (7 6 5 4 3)						
3d3	(4Fe)	3/2	4d	3	−2.37021E+00	3.25	5 PDFGH e
3d3	(4Fe)	5/2	4d	4	−2.36647E+00	3.25	5 DFGH e
3d3	(4Fe)	5/2	4d	5	−2.36189E+00	3.25	5 FGH e
3d3	(4Fe)	3/2	4d	1	−2.35988E+00	3.25	5 PDF e
3d3	(4Fe)	7/2	4d	6	−2.35651E+00	3.25	5 GH e
3d3	(4Fe)	5/2	4d	2	−2.35541E+00	3.26	5 PDFG e
3d3	(4Fe)	9/2	4d	7	−2.35041E+00	3.25	5 H e
3d3	(4Fe)	5/2	4d	1	−2.34932E+00	3.26	5 PDF e
3d3	(4Fe)	9/2	4d	3	−2.34736E+00	3.25	5 PDFGH e
3d3	(4Fe)	9/2	4d	3	−2.34736E+00	3.25	5 PDFGH e
3d3	(4Fe)	7/2	4d	2	−2.34633E+00	3.26	5 PDFG e
3d3	(4Fe)	3/2	4d	2	−2.34397E+00	3.27	5 PDFG e
3d3	(4Fe)	7/2	4d	4	−2.34329E+00	3.26	5 DFGH e
3d3	(4Fe)	5/2	4d	3	−2.34092E+00	3.26	5 PDFGH e
3d3	(4Fe)	9/2	4d	3	−2.33989E+00	3.26	5 PDFGH e
3d3	(4Fe)	9/2	4d	5	−2.33822E+00	3.26	5 FGH e
3d3	(4Fe)	7/2	4d	5	−2.33234E+00	3.27	5 FGH e
3d3	(4Fe)	9/2	4d	6	−2.32699E+00	3.26	5 GH e
3d3	(4Fe)	3/2	4d	4	−2.28772E+00	3.31	5 DFGH e
3d3	(4Fe)	3/2	4d	0	−2.28673E+00	3.31	5 D e
3d3	(4Fe)	7/2	4d	1	−2.28265E+00	3.30	5 PDF e
3d3	(4Fe)	9/2	4d	2	−2.27468E+00	3.30	5 PDFG e
3d3	(4Fe)	7/2	4d	3	−2.26346E+00	3.31	5 PDFGH e
3d3	(4Fe)	9/2	4d	4	−2.25835E+00	3.31	5 DFGH e
Ncal = 23: set complete							
Nlv = 3, 1,e:	P (1) D (2) F (3)						
3d3	(2Pe)	3/2	4d	1	−2.08815E+00	3.26	1 P e
3d3	(2Pe)	1/2	4d	2	−1.95699E+00	3.41	1 D e
3d3	(2Pe)	3/2	4d	3	−1.94667E+00	3.38	1 F e
Ncal = 3: set complete							
Nlv = 15, 3,e:	P (2 1 0) D (3 2 1) F (4 3 2) G (5 4 3) H (6 5 4)						
3d3	(4Fe)	3/2	4d	1	−2.35634E+00	3.26	3 PD e
3d3	(4Fe)	5/2	4d	2	−2.35219E+00	3.25	3 PDF e
3d3	(4Fe)	7/2	4d	3	−2.34872E+00	3.25	3 DFG e
3d3	(4Fe)	5/2	4d	4	−2.33701E+00	3.27	3 FGH e
3d3	(4Fe)	5/2	4d	5	−2.28113E+00	3.31	3 GH e
3d3	(4Fe)	3/2	4d	3	−2.28060E+00	3.31	3 DFG e
3d3	(4Fe)	7/2	4d	4	−2.27417E+00	3.31	3 FGH e
3d3	(4Fe)	9/2	4d	6	−2.27323E+00	3.30	3 H e
3d3	(4Fe)	3/2	4d	2	−2.26789E+00	3.32	3 PDF e
3d3	(4Fe)	7/2	4d	5	−2.26632E+00	3.31	3 GH e
3d3	(4Fe)	5/2	4d	0	−2.24585E+00	3.33	3 P e
3d3	(4Fe)	5/2	4d	1	−2.24483E+00	3.33	3 PD e
3d3	(4Fe)	7/2	4d	2	−2.24278E+00	3.33	3 PDF e
3d3	(4Fe)	7/2	4d	3	−2.23973E+00	3.33	3 DFG e
3d3	(4Fe)	9/2	4d	4	−2.23571E+00	3.33	3 FGH e

Table 1. continued

C_t	$S_tL_t\pi_t$	J_t	nl	J	E(cal)	ν	$SL\pi$
Ncal = 15: set complete							
Nlv = 13, 3,e:	S (1) P (2 1 0) D (3 2 1) F (4 3 2) G (5 4 3)						
3d3 2	(2De)	5/2	5d	1	−1.05446E+00	4.36	3 SPD e
3d3 2	(2De)	5/2	5d	5	−1.04247E+00	4.38	3 G e
3d3 2	(2De)	3/2	5d	3	−1.04179E+00	4.38	3 DFG e
3d3 2	(2De)	3/2	5d	1	−1.03332E+00	4.40	3 SPD e
3d3 2	(2De)	5/2	5d	4	−1.03014E+00	4.40	3 FG e
3d3 2	(2De)	5/2	5d	2	−1.02889E+00	4.40	3 PDF e
3d3 2	(2De)	3/2	5d	0	−1.02130E+00	4.42	3 P e
3d3 2	(2De)	5/2	5d	1	−1.01682E+00	4.43	3 SPD e
3d3 2	(2De)	5/2	5d	3	−1.01420E+00	4.43	3 DFG e
3d3 2	(2De)	3/2	5d	2	−1.00936E+00	4.44	3 PDF e
3d3 2	(2De)	3/2	5d	2	−9.92578E-01	4.47	3 PDF e
3d3 2	(2De)	5/2	5d	3	−9.81500E-01	4.49	3 DFG e
Ncal = 12 , Nlv = 13: set incomplete, level missing: 4							

usually the lowest. For example, of the two $J = 4$ levels with terms ^{3}(F,G) in the second set, the first or the lower level could be ^{3}G while the second or the higher one could be ^{3}F. It may be noted that this criterion is violated for a number of cases in Fe V due to strong CI. In Table 1b, the upper sets of low energies are complete. The two lower sets are incomplete where a few levels are missing. The missing levels are detected by the program PRCBPID.

4.1.3. Comparison with observed energies

Only a limited number of observed energy levels of Fe V are available (Sugar & Corliss 1985). All 179 observed levels were identified in a straightforward manner by the program PRCBPID. The present results are found to agree to about 1% with the observed energies for most of the levels (Table III, Nahar & Pradhan 2000). In Table 2, a comparison is presented for the $3d^4$ levels. The experimentally observed levels are also the lowest calculated levels in Fe V. The additional information in Table 2 is the level index, I_J, next to the J-values. As the BPRM levels are designated with $J\pi$ values only, the level index shows the energy position, in ascending order, of the level in the $J\pi$ symmetry. It is necessary to use the level indices to make the correspondence among the calculated and the observed levels for later use.

Although the LS term designation in general meets consistency checks, it is possible that there is some uncertainty in the designations. The spin multiplicities of the ion are obtained by the addition of the angular momentum 1/2 of the outer electron to the total spin, S_t, of the target. The higher multiplicity corresponds to the addition of +1/2, and the lower one to the subtraction of −1/2. Typically the level with higher multiplicity lies lower. Due to the large number of different channels representing the levels of a $J\pi$ symmetry, it is possible that this angular addition might have been interchanged for some cases where the channels themselves are incorrectly identified. Therefore, for example, a triplet could be represented by a singlet and vice versa. This can affect the L designation since a singlet can be assigned only to one single total L, whereas a triplet can be assigned to a few possible L values. For such cases, the LS multiplets may not represent the correct transitions.

We emphasize, however, that the present calculations are all in intermediate coupling and the LS coupling designations attempted in this work are carried out only to complete the full spectroscopic identification that may be of interest for (a) specialized users such as experimentalists, and (b) as a record of all possible information (some of which may be uncertain) that can be derived from the BPRM calculations for bound levels.

4.2. E1 oscillators strengths from the BPRM calculations

The bound-bound transitions among the 3865 fine-structure levels of Fe V have resulted in 1.46 10^6 oscillator strengths for dipole-allowed and intercombination transitions.

4.2.1. Calculated f-values for the allowed transitions

Table 3 presents a partial set, in the format adopted, from the complete file of oscillator strengths. The two numbers at the beginning of the table are the nuclear charge (i.e. Z = 26) and the number of electrons (N_{elc} = 22) for Fe V. Below this line are the sets of transitions of a pair of symmetries $J\pi$ − $J'\pi'$. The first line of each set contains values of $2J$, parity π (=0 for even and =1 for odd), $2J'$ and π'. Hence in Table 3, the set of transitions given are among $J = 0^e$ − $J = 1^\circ$. The line following the transition symmetries specifies the number of bound levels, N_{Ji} and N_{Jj}, of the symmetries among which the transitions occur. This line is followed by $N_{Ji} \times N_{Jj}$ transitions.

The first two columns are the level indices, I_i and I_j (as mentioned above) for the energy indices of the levels, and the third and the fourth columns are their energies, E_i and E_j, in Rydberg units. The fifth and sixth columns are gf_L and gf_V, where f_L and f_V are the oscillator strengths in length and velocity forms, and $g = 2J+1$ (J is the total angular momentum of the lower level). For the gf-values that are negative the lower level is i (absorption) and for the positive ones the lower level is j (emission). The last column gives the transition probability, $A_{ji}(\mathrm{s}^{-1})$. To obtain the identification of the levels, Table 1a should be referrred to following I_i and I_j. For example, the second transition of Table 3 corresponds to the intercombination transition $3d^4(^5D^e)(I_i = 1) \rightarrow 3d^3(^4F^e)4p(^3D^\circ)(I_j = 3)$.

4.2.2. f-values with experimental energies

As the observed energies are much more precisely known that the calculated ones, the f and A-values can be reprocessed with the observed energies for some improvement in accuracy. Using the energy independent BPRM line strength, S (Eq. 7), the f-value can be obtained as,

$$f_{ij} = S(i, j, \mathrm{BPRM})\frac{E_{ji}(\mathrm{obs})}{(3g_i)}. \quad (13)$$

Transitions among all observed levels have been so reprocessed. This recalculated subset consists of 3737 dipole-allowed and intercombination transitions among the 179 observed levels (a relatively small part of the present transition probabilities dataset). The calculated energy level indices corresponding to the observed levels for each $J\pi$ are listed in Table 4.

A sample set of f- and A-values from the reprocessed transitions are presented in Table 5a in $J\pi - J'\pi'$ order. Each transition is given with complete identification. The level index, I_i, for each energy level is given next to the J-value for easy linkage to the energy and f-files. In all calculations where large number of transitions are used, the reprocessed f- and A-values should replace those in the complete file (containing 1.46 10^6 transitions). For example, the f- and A-values for the first transition $J = 0^e(I_i = 1) \rightarrow J = 1^\circ(I_j = 1)$ in Table 3 should be replaced by those for the first transition in Table 5a. The overall replacement of transitions can be carried out easily using the level energy index set in Table 4.

4.2.3. Spectroscopic designation and completeness

The reprocessed transitions are further ordered in terms of their configurations for a completeness check, and to obtain the LS multiplet designations. A partial set is presented in Table 5b (the complete table is available electronically). The completeness depends on the observed set of fine-structure levels since transitions have been reprocessed only for the observed levels. The LS multiplets are useful for various comparisons with existing values where fine-structure transitions can not be resolved.

Table 2. Comparison of calculated BPRM energies, E_c, with the observed ones (Sugar & Corliss 1985), E_o, of Fe V. I_J is the level index for the energy position in symmetry $J\pi$

Level		J	I_J	E_c(Ry)	E_o(Ry)
$3d^4$	^{5}D	4	1	5.5493	5.5015
$3d^4$	^{5}D	3	1	5.5542	5.5058
$3d^4$	^{5}D	2	1	5.5580	5.5094
$3d^4$	^{5}D	1	1	5.5607	5.5119
$3d^4$	^{5}D	0	1	5.5621	5.5132
$3d^42$	^{3}P	2	2	5.3247	5.2720
$3d^42$	^{3}P	1	2	5.3389	5.2856
$3d^42$	^{3}P	0	2	5.3471	5.2940
$3d^4$	^{3}H	6	1	5.3074	5.2805
$3d^4$	^{3}H	5	1	5.3111	5.2833
$3d^4$	^{3}H	4	2	5.3143	5.2860
$3d^42$	^{3}F	4	3	5.3043	5.2674
$3d^42$	^{3}F	3	2	5.3064	5.2686
$3d^42$	^{3}F	2	3	5.3076	5.2693
$3d^4$	^{3}G	5	2	5.2581	5.2359
$3d^4$	^{3}G	4	4	5.2614	5.2384
$3d^4$	^{3}G	3	3	5.2651	5.2415
$3d^42$	^{1}G	4	5	5.2006	5.1798
$3d^4$	^{3}D	3	4	5.1950	5.1794
$3d^4$	^{3}D	2	4	5.1945	5.1782
$3d^4$	^{3}D	1	3	5.1928	5.1767
$3d^4$	^{1}I	6	2	5.1852	5.1713
$3d^42$	^{1}S	0	3	5.1700	5.1520
$3d^42$	^{1}D	2	5	5.1353	5.0913
$3d^4$	^{1}F	3	5	5.0476	5.0326
$3d^41$	^{3}P	2	6	4.9756	4.9495
$3d^41$	^{3}P	1	4	4.9663	4.9398
$3d^41$	^{3}P	0	4	4.9616	4.9352
$3d^41$	^{3}F	4	6	4.9719	4.9460
$3d^41$	^{3}F	3	6	4.9706	4.9449
$3d^41$	^{3}F	2	7	4.9712	4.9453
$3d^41$	^{1}G	4	7	4.8830	4.8636
$3d^41$	^{1}D	2	8	4.6609	4.6581
$3d^41$	^{1}S	0	5	4.4302	4.4093

Semi-empirical atomic structure calculations have been carried out be other workers (Fawcett 1989; Quinet & Hansen 1995). Present oscillator strengths are compared with available calculations by Fawcett (1989), the LS coupling R-matrix calculations from the OP (Butler, TOPbase 1993) and from the IP (Bautista 1996), for some low lying transitions. Comparison in Table 5b shows various degrees of agreement. Present f-values agree very well (within 10%) with those by Fawcett for some fine-structure transitions while disagree considerably with the others within the same LS multiplet. For example, the agreement is good for most of the fine-structure transitions of $3d^4(^5D) \rightarrow 3d^3(^4F)4p(^5D^\circ)$, $3d^4(^5D) \rightarrow 3d^3(^4P)4p(^5P^\circ)$, and $3d^42(^3P) \rightarrow 3d^3(^4F)4p(^3D^\circ)$ while the disagreement is large with other as well as with those of $3d^4(^5D) \rightarrow 3d^3(^4F)4p(^5F^\circ)$. The agreement of the present LS multiplets with the others is good for strong transitions such as $3d^4(^5D) \rightarrow 3d^3(^4F)4p(^5F^\circ,^5D^\circ,^5P^\circ)$, and $3d^42(^3P) \rightarrow 3d^3(^4F)4p(^3D^\circ)$, but is poor for the weak ones.

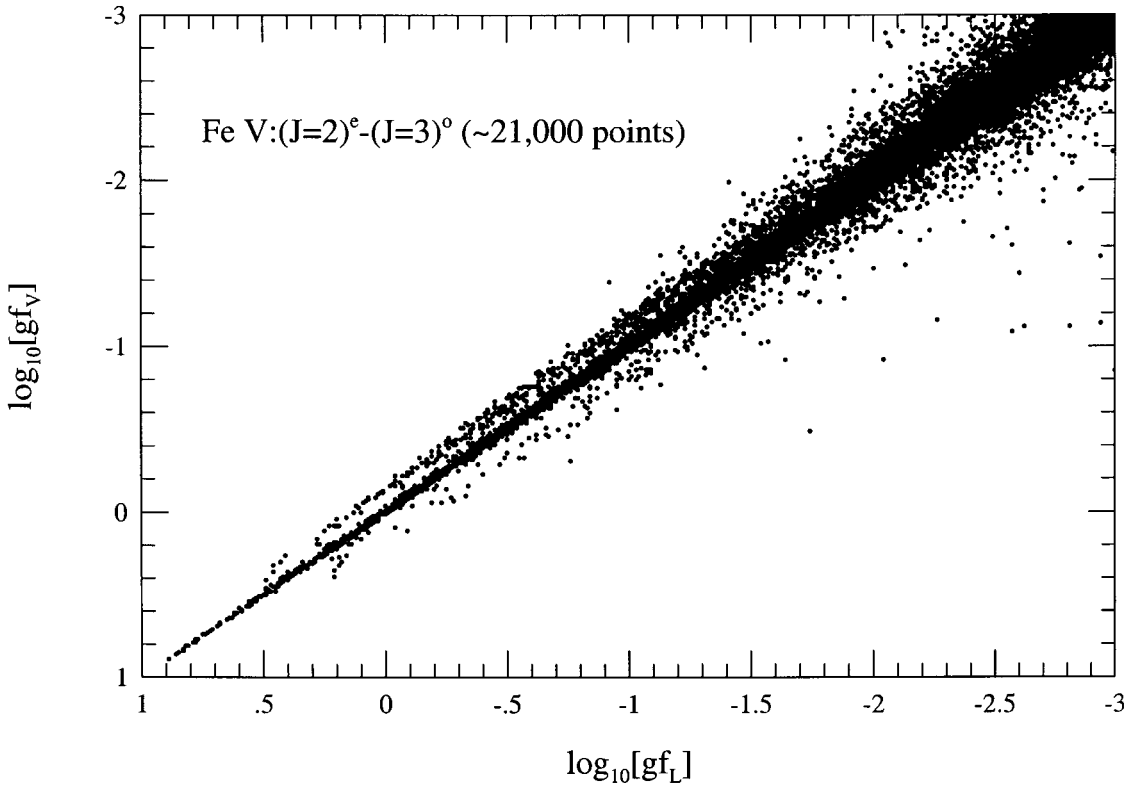

Fig. 1. Comparison between the length and the velocity forms of f-values for $(J=2)^{\rm e}-(J=3)^3$ transitions in Fe V

4.2.4. Estimate of uncertainties

The uncertainties of the BPRM transition probabilities for the allowed transitons are expected to be within 10% for the strong transitions, and $10-30\%$ for the weak ones. A measure of the uncertainty can be obtained from the dispersion of the f-values in length and velocity forms, which generally indicate deviations from the "exact" wavefunctions (albeit with some exceptions). Figure 1 presents a plot of $\log_{10}gf$ values, length vs. velocity, for the transitions $(J=2)^{\rm e}-(J=3)^3$ of Fe V. Though most of the points lie close to the $gf_L = gf_V$ line, significant dispersion is seen for gf values smaller than 0.01. We should note that the level of uncertainty may in fact be less than the dispersion shown in Fig. 1; in the close coupling R-matrix calculations the length formulation is likely to be more accurate than the velocity formulaton since the wavefunctions are better represented in the asymptotic region that dominates the contribution to the length form of the oscillator strength.

4.3. Forbidden transition probabilities

The transition probabilities, $A^{\rm q}$ and $A^{\rm m}$, for 362 forbidden E2 and M1 transitions are obtained using some semi-empirical corrections. The $A^{\rm q}$ in general are much smaller than the $A^{\rm m}$. Although $A^{\rm q}$ is smaller, there are many cases where one or the other is negligible. Owing to the widespread use of the only other previous calculation by Garstang (1957), it is important to establish the general level of differences with the previous work. Table 6 gives a detailed comparison. The agreement between the two sets of data is generally good with a few noticeable discrepancies.

A partial set of the transition probabilities are given in Table 7 along with the observed wavelengths in microns. The full Table of forbidden transition probabilities is available electronically.

5. Conclusion

To exemplify the future potential of computational spectroscopy with the Breit-Pauli R-matrix method, complemented by related atomic structure calculations, we present a fairly complete and large-scale set of mainly ab initio transition probabilities for a complex atomic system. Level energies and fine-structure transition probabilities for Fe V are presented in a comprehensive manner with spectroscopic identifications. We should expect these data to be particularly useful for the calculation of monochromatic opacities and in the analysis of spectra from astrophysical and laboratory sources where non-local thermodynamic equilibrium (NLTE) atomic models with many excited levels are needed.

Table 3. Transition probabilities for Fe V (see text for explanation)

26	22					
0	0	2	1			
80	236	E_i(Ry)	E_j(Ry)	gf_L	gf_V	A_{ji}(s^{-1})
1	1	−5.56210E+00	−3.14950E+00	−2.212E-01	−1.800E-01	3.447E+09
1	2	−5.56210E+00	−3.14082E+00	−5.660E-03	−4.178E-03	8.884E+07
1	3	−5.56210E+00	−3.13088E+00	−5.894E-02	−4.843E-02	9.328E+08
1	4	−5.56210E+00	−2.99367E+00	−8.675E-02	−7.425E-02	1.532E+09
1	5	−5.56210E+00	−2.97465E+00	−4.542E-03	−4.060E-03	8.142E+07
1	6	−5.56210E+00	−2.96345E+00	−8.619E-05	−1.086E-04	1.558E+06
1	7	−5.56210E+00	−2.93263E+00	−1.059E-03	−8.938E-04	1.961E+07
1	8	−5.56210E+00	−2.90308E+00	−1.333E-08	−3.023E-07	2.524E+02
1	9	−5.56210E+00	−2.88417E+00	−2.099E-06	−9.150E-07	4.031E+04
1	10	−5.56210E+00	−2.87902E+00	−1.268E-03	−9.286E-04	2.444E+07
1	11	−5.56210E+00	−2.86205E+00	−4.284E-06	−4.003E-06	8.362E+04
1	12	−5.56210E+00	−2.84777E+00	−4.484E-06	−5.049E-06	8.845E+04
1	13	−5.56210E+00	−2.83128E+00	−3.114E-05	−2.131E-05	6.217E+05
1	14	−5.56210E+00	−2.78217E+00	−2.470E-06	−1.789E-06	5.111E+04
1	15	−5.56210E+00	−2.77047E+00	−6.248E-05	−4.283E-05	1.304E+06
1	16	−5.56210E+00	−2.65585E+00	−4.772E-06	−4.614E-06	1.079E+05
1	17	−5.56210E+00	−2.49355E+00	−4.898E-06	−5.125E-06	1.235E+05
1	18	−5.56210E+00	−2.41413E+00	−3.274E-07	−6.115E-07	8.688E+03
1	19	−5.56210E+00	−2.33944E+00	−2.223E-09	−4.905E-09	6.181E+01
1	20	−5.56210E+00	−1.68531E+00	−1.110E-02	−7.389E-03	4.466E+08
1	21	−5.56210E+00	−1.68346E+00	−1.821E-02	−1.320E-02	7.334E+08
1	22	−5.56210E+00	−1.67450E+00	−9.466E-05	−9.518E-05	3.830E+06
1	23	−5.56210E+00	−1.59625E+00	−5.222E-03	−3.143E-03	2.199E+08
1	24	−5.56210E+00	−1.59532E+00	−1.810E-03	−1.229E-03	7.624E+07
1	25	−5.56210E+00	−1.58926E+00	−1.444E-03	−1.553E-03	6.100E+07
1	26	−5.56210E+00	−1.58695E+00	−2.143E-01	−1.527E-01	9.066E+09
1	27	−5.56210E+00	−1.58282E+00	−1.247E-01	−8.966E-02	5.285E+09
1	28	−5.56210E+00	−1.56818E+00	−3.245E-03	−2.354E-03	1.386E+08
1	29	−5.56210E+00	−1.52505E+00	−1.908E-02	−1.419E-02	8.326E+08
1	30	−5.56210E+00	−1.51857E+00	−4.315E-03	−3.201E-03	1.889E+08
1	31	−5.56210E+00	−1.51106E+00	−9.942E-04	−7.265E-04	4.369E+07
1	32	−5.56210E+00	−1.48630E+00	−1.718E-05	−1.163E-05	7.641E+05
1	33	−5.56210E+00	−1.45506E+00	−1.579E-04	−1.075E-04	7.130E+06
1	34	−5.56210E+00	−1.45100E+00	−7.533E-06	−4.042E-06	3.409E+05
1	35	−5.56210E+00	−1.44432E+00	−5.868E-04	−3.975E-04	2.664E+07
1	36	−5.56210E+00	−1.44049E+00	−1.021E-01	−7.036E-02	4.642E+09
1	37	−5.56210E+00	−1.43765E+00	−3.304E-04	−2.278E-04	1.505E+07
1	38	−5.56210E+00	−1.43257E+00	−3.309E-05	−2.303E-05	1.511E+06
1	39	−5.56210E+00	−1.42555E+00	−2.467E-07	−1.329E-07	1.130E+04
1	40	−5.56210E+00	−1.41678E+00	−2.418E-05	−1.832E-05	1.112E+06
1	41	−5.56210E+00	−1.41009E+00	−1.689E-02	−1.254E-02	7.797E+08
1	42	−5.56210E+00	−1.40208E+00	−5.592E-05	−3.657E-05	2.591E+06
1	43	−5.56210E+00	−1.40135E+00	−1.642E-05	−1.154E-05	7.613E+05
1	44	−5.56210E+00	−1.39712E+00	−1.010E-04	−6.246E-05	4.691E+06
1	45	−5.56210E+00	−1.39057E+00	−1.312E-05	−9.621E-06	6.115E+05
1	46	−5.56210E+00	−1.37572E+00	−1.298E-05	−8.241E-06	6.089E+05
1	47	−5.56210E+00	−1.36381E+00	−1.730E-04	−1.098E-04	8.166E+06
1	48	−5.56210E+00	−1.34841E+00	−5.225E-07	−1.695E-06	2.484E+04
1	49	−5.56210E+00	−1.33149E+00	−2.354E-06	−1.675E-06	1.128E+05
1	50	−5.56210E+00	−1.32616E+00	−5.604E-05	−3.284E-05	2.692E+06

Table 4. Calculated energy level indices for various $J\pi$ symmetries; allowed transitions among all these levels have been reprocessed using observed energies. n_j is the total number of $J\pi$ levels observed

$J\pi$	n_j	level indices
0 e	6	1,2,3,4,5,6
0 o	6	1,2,3,4,6,7
1 e	11	1,2,3,4,5,6,7,8,9,10,11
1 o	19	1,2,3,4,5,6,7,8,9,10,11,12,13,14,15,16,17,18,19
2 e	18	1,2,3,4,5,6,7,8,9,10,11,12,13,14,15,16,17,18
2 o	24	1,2,3,4,5,6,7,8,9,10,11,12,13,14,15,17,18,19,20,21,22,23,24,25
3 e	14	1,2,3,4,5,6,7,8,9,10,11,12,13,14
3 o	24	1,2,3,4,5,6,7,8,9,10,11,12,13,14,15,16,17,18,19,20,21,22,23,24
4 e	13	1,2,3,4,5,6,7,8,9,10,11,12,13
4 o	18	1,2,3,4,5,6,7,8,9,10,11,12,13,14,15,16,17,18
5 e	6	1,2,3,4,5,6
5 o	11	1,2,3,4,5,6,7,8,9,10,11
6 e	3	1,2,3
6 o	5	1,2,3,4,5
7 o	1	1

Table 5. a) Sample set of reprocessed f- and A-values with observed transition energies. I_i and I_j are the level indices

C_i	C_j	$S_iL_i\pi_i$	$S_jL_j\pi_j$	$2J_i+1$	I_i	$2J_j+1$	I_j	E_i(Ry)	E_j(Ry)	f	$A(s^{-1})$
$3d^4$	$-3d^3(4F)4p$	$^5D^e$	$^5D^\circ$	1	1	3	2	5.5132	3.1540	5.515E-03	8.22E+07
$3d^4$	$-3d^3(4F)4p$	$^5D^e$	$^3D^\circ$	1	1	3	3	5.5132	3.1439	5.744E-02	8.63E+08
$3d^4$	$-3d^3(4P)4p$	$^5D^e$	$^5P^\circ$	1	1	3	4	5.5132	3.0195	8.420E-02	1.40E+09
$3d^4$	$-3d^3(4P)4p$	$^5D^e$	$^5D^\circ$	1	1	3	5	5.5132	3.0058	4.401E-03	7.41E+07
$3d^4$	$-3d^3(4P)4p$	$^5D^e$	$^3P^\circ$	1	1	3	6	5.5132	2.9911	8.365E-05	1.42E+06
$3d^4$	$-3d^3(2P)4p$	$^5D^e$	$^3P^\circ$	1	1	3	7	5.5132	2.9439	1.035E-03	1.83E+07
$3d^4$	$-3d^3(2D2)4p$	$^5D^e$	$^1P^\circ$	1	1	3	8	5.5132	2.9073	1.306E-08	2.38E+02
$3d^4$	$-3d^3(2D2)4p$	$^5D^e$	$^3D^\circ$	1	1	3	9	5.5132	2.8826	2.062E-06	3.82E+04
$3d^4$	$-3d^3(2P)4p$	$^5D^e$	$^3D^\circ$	1	1	3	10	5.5132	2.9274	1.222E-03	2.19E+07
$3d^4$	$-3d^3(2P)4p$	$^5D^e$	$^3S^\circ$	1	1	3	11	5.5132	2.9052	4.138E-06	7.54E+04
$3d^4$	$-3d^3(4P)4p$	$^5D^e$	$^3D^\circ$	1	1	3	12	5.5132	2.8991	4.318E-06	7.90E+04
$3d^4$	$-3d^3(2D2)4p$	$^5D^e$	$^3P^\circ$	1	1	3	13	5.5132	2.8652	3.020E-05	5.67E+05
$3d^4$	$-3d^3(2P)4p$	$^5D^e$	$^1P^\circ$	1	1	3	14	5.5132	2.8161	2.397E-06	4.67E+04
$3d^4$	$-3d^3(4P)4p$	$^5D^e$	$^3S^\circ$	1	1	3	15	5.5132	2.8282	6.009E-05	1.16E+06
$3d^4$	$-3d^3(2F)4p$	$^5D^e$	$^3D^\circ$	1	1	3	16	5.5132	2.7003	4.619E-06	9.78E+04
$3d^4$	$-3d^3(2D1)4p$	$^5D^e$	$^3D^\circ$	1	1	3	17	5.5132	2.5285	4.765E-06	1.14E+05
$3d^4$	$-3d^3(2D1)4p$	$^5D^e$	$^3P^\circ$	1	1	3	18	5.5132	2.4580	3.177E-07	7.94E+03
$3d^4$	$-3d^3(2D1)4p$	$^5D^e$	$^1P^\circ$	1	1	3	19	5.5132	2.3924	2.152E-09	5.61E+01
$3d^42$	$-3d^3(4F)4p$	$^3P^e$	$^5F^\circ$	1	2	3	1	5.2940	3.1644	2.317E-02	2.81E+08
$3d^42$	$-3d^3(4F)4p$	$^3P^e$	$^5D^\circ$	1	2	3	2	5.2940	3.1540	1.751E-02	2.15E+08
$3d^42$	$-3d^3(4F)4p$	$^3P^e$	$^3D^\circ$	1	2	3	3	5.2940	3.1439	6.702E-02	8.29E+08
$3d^42$	$-3d^3(4P)4p$	$^3P^e$	$^5P^\circ$	1	2	3	4	5.2940	3.0195	7.726E-05	1.07E+06
$3d^42$	$-3d^3(4P)4p$	$^3P^e$	$^5D^\circ$	1	2	3	5	5.2940	3.0058	2.863E-03	4.01E+07
$3d^42$	$-3d^3(4P)4p$	$^3P^e$	$^3P^\circ$	1	2	3	6	5.2940	2.9911	1.907E-02	2.71E+08
$3d^42$	$-3d^3(2P)4p$	$^3P^e$	$^3P^\circ$	1	2	3	7	5.2940	2.9439	9.377E-02	1.39E+09
$3d^42$	$-3d^3(2D2)4p$	$^3P^e$	$^1P^\circ$	1	2	3	8	5.2940	2.9073	6.430E-03	9.81E+07
$3d^42$	$-3d^3(2D2)4p$	$^3P^e$	$^3D^\circ$	1	2	3	9	5.2940	2.8826	7.067E-03	1.10E+08
$3d^42$	$-3d^3(2P)4p$	$^3P^e$	$^3D^\circ$	1	2	3	10	5.2940	2.9274	7.538E-02	1.13E+09
$3d^42$	$-3d^3(2P)4p$	$^3P^e$	$^3S^\circ$	1	2	3	11	5.2940	2.9052	2.193E-03	3.35E+07
$3d^42$	$-3d^3(4P)4p$	$^3P^e$	$^3D^\circ$	1	2	3	12	5.2940	2.8991	3.284E-02	5.04E+08
$3d^42$	$-3d^3(2D2)4p$	$^3P^e$	$^3P^\circ$	1	2	3	13	5.2940	2.8652	6.023E-03	9.51E+07
$3d^42$	$-3d^3(2P)4p$	$^3P^e$	$^1P^\circ$	1	2	3	14	5.2940	2.8161	1.578E-04	2.59E+06
$3d^42$	$-3d^3(4P)4p$	$^3P^e$	$^3S^\circ$	1	2	3	15	5.2940	2.8282	2.772E-04	4.51E+06
$3d^42$	$-3d^3(2F)4p$	$^3P^e$	$^3D^\circ$	1	2	3	16	5.2940	2.7003	1.347E-03	2.43E+07
$3d^42$	$-3d^3(2D1)4p$	$^3P^e$	$^3D^\circ$	1	2	3	17	5.2940	2.5285	4.641E-03	9.50E+07
$3d^42$	$-3d^3(2D1)4p$	$^3P^e$	$^3P^\circ$	1	2	3	18	5.2940	2.4580	3.200E-04	6.89E+06
$3d^42$	$-3d^3(2D1)4p$	$^3P^e$	$^1P^\circ$	1	2	3	19	5.2940	2.3924	1.102E-05	2.48E+05
$3d^42$	$-3d^3(4F)4p$	$^1S^e$	$^5F^\circ$	1	3	3	1	5.1520	3.1644	7.493E-06	7.93E+04
$3d^42$	$-3d^3(4F)4p$	$^1S^e$	$^5D^\circ$	1	3	3	2	5.1520	3.1540	7.672E-06	8.20E+04
$3d^42$	$-3d^3(4F)4p$	$^1S^e$	$^3D^\circ$	1	3	3	3	5.1520	3.1439	2.529E-05	2.73E+05
$3d^42$	$-3d^3(4P)4p$	$^1S^e$	$^5P^\circ$	1	3	3	4	5.1520	3.0195	1.024E-05	1.25E+05
$3d^42$	$-3d^3(4P)4p$	$^1S^e$	$^5D^\circ$	1	3	3	5	5.1520	3.0058	1.932E-04	2.38E+06
$3d^42$	$-3d^3(4P)4p$	$^1S^e$	$^3P^\circ$	1	3	3	6	5.1520	2.9911	2.404E-05	3.01E+05
$3d^42$	$-3d^3(2P)4p$	$^1S^e$	$^3P^\circ$	1	3	3	7	5.1520	2.9439	7.035E-03	9.18E+07
$3d^42$	$-3d^3(2D2)4p$	$^1S^e$	$^1P^\circ$	1	3	3	8	5.1520	2.9073	8.021E-03	1.08E+08
$3d^42$	$-3d^3(2D2)4p$	$^1S^e$	$^3D^\circ$	1	3	3	9	5.1520	2.8826	2.263E-01	3.12E+09
$3d^42$	$-3d^3(2P)4p$	$^1S^e$	$^3D^\circ$	1	3	3	10	5.1520	2.9274	1.305E-03	1.73E+07
$3d^42$	$-3d^3(2P)4p$	$^1S^e$	$^3S^\circ$	1	3	3	11	5.1520	2.9052	1.968E-04	2.66E+06
$3d^42$	$-3d^3(4P)4p$	$^1S^e$	$^3D^\circ$	1	3	3	12	5.1520	2.8991	2.048E-03	2.78E+07
$3d^42$	$-3d^3(2D2)4p$	$^1S^e$	$^3P^\circ$	1	3	3	13	5.1520	2.8652	1.148E-02	1.61E+08
$3d^42$	$-3d^3(2P)4p$	$^1S^e$	$^1P^\circ$	1	3	3	14	5.1520	2.8161	7.864E-02	1.15E+09
$3d^42$	$-3d^3(4P)4p$	$^1S^e$	$^3S^\circ$	1	3	3	15	5.1520	2.8282	2.714E-02	3.92E+08
$3d^42$	$-3d^3(2F)4p$	$^1S^e$	$^3D^\circ$	1	3	3	16	5.1520	2.7003	5.453E-07	8.78E+03
$3d^42$	$-3d^3(2D1)4p$	$^1S^e$	$^3D^\circ$	1	3	3	17	5.1520	2.5285	6.569E-05	1.21E+06
$3d^42$	$-3d^3(2D1)4p$	$^1S^e$	$^3P^\circ$	1	3	3	18	5.1520	2.4580	2.050E-07	3.98E+03
$3d^42$	$-3d^3(2D1)4p$	$^1S^e$	$^1P^\circ$	1	3	3	19	5.1520	2.3924	2.421E-04	4.94E+06
$3d^41$	$-3d^3(4F)4p$	$^3P^e$	$^5F^\circ$	1	4	3	1	4.9352	3.1644	9.362E-05	7.86E+05
$3d^41$	$-3d^3(4F)4p$	$^3P^e$	$^5D^\circ$	1	4	3	2	4.9352	3.1540	2.852E-05	2.42E+05
$3d^41$	$-3d^3(4F)4p$	$^3P^e$	$^3D^\circ$	1	4	3	3	4.9352	3.1439	1.131E-04	9.72E+05
$3d^41$	$-3d^3(4P)4p$	$^3P^e$	$^5P^\circ$	1	4	3	4	4.9352	3.0195	4.206E-04	4.13E+06
$3d^41$	$-3d^3(4P)4p$	$^3P^e$	$^5D^\circ$	1	4	3	5	4.9352	3.0058	1.295E-02	1.29E+08
$3d^41$	$-3d^3(4P)4p$	$^3P^e$	$^3P^\circ$	1	4	3	6	4.9352	2.9911	1.009E-02	1.02E+08
$3d^41$	$-3d^3(2P)4p$	$^3P^e$	$^3P^\circ$	1	4	3	7	4.9352	2.9439	7.813E-03	8.29E+07
$3d^41$	$-3d^3(2D2)4p$	$^3P^e$	$^1P^\circ$	1	4	3	8	4.9352	2.9073	3.255E-04	3.58E+06
$3d^41$	$-3d^3(2D2)4p$	$^3P^e$	$^3D^\circ$	1	4	3	9	4.9352	2.8826	3.644E-04	4.11E+06
$3d^41$	$-3d^3(2P)4p$	$^3P^e$	$^3D^\circ$	1	4	3	10	4.9352	2.9274	2.974E-03	3.21E+07
$3d^41$	$-3d^3(2P)4p$	$^3P^e$	$^3S^\circ$	1	4	3	11	4.9352	2.9052	2.856E-04	3.15E+06
$3d^41$	$-3d^3(4P)4p$	$^3P^e$	$^3D^\circ$	1	4	3	12	4.9352	2.8991	4.236E-04	4.70E+06
$3d^41$	$-3d^3(2D2)4p$	$^3P^e$	$^3P^\circ$	1	4	3	13	4.9352	2.8652	5.201E-02	5.97E+08
$3d^41$	$-3d^3(2P)4p$	$^3P^e$	$^1P^\circ$	1	4	3	14	4.9352	2.8161	1.028E-02	1.24E+08
$3d^41$	$-3d^3(4P)4p$	$^3P^e$	$^3S^\circ$	1	4	3	15	4.9352	2.8282	4.824E-02	5.73E+08
$3d^41$	$-3d^3(2F)4p$	$^3P^e$	$^3D^\circ$	1	4	3	16	4.9352	2.7003	1.648E-01	2.20E+09
$3d^41$	$-3d^3(2D1)4p$	$^3P^e$	$^3D^\circ$	1	4	3	17	4.9352	2.5285	2.144E-08	3.33E+02
$3d^41$	$-3d^3(2D1)4p$	$^3P^e$	$^3P^\circ$	1	4	3	18	4.9352	2.4580	4.867E-02	8.00E+08
$3d^41$	$-3d^3(2D1)4p$	$^3P^e$	$^1P^\circ$	1	4	3	19	4.9352	2.3924	4.875E-05	8.44E+05
$3d^41$	$-3d^3(4F)4p$	$^1S^e$	$^5F^\circ$	1	5	3	1	4.4093	3.1644	8.262E-08	3.43E+02
$3d^41$	$-3d^3(4F)4p$	$^1S^e$	$^5D^\circ$	1	5	3	2	4.4093	3.1540	3.663E-08	1.55E+02
$3d^41$	$-3d^3(4F)4p$	$^1S^e$	$^3D^\circ$	1	5	3	3	4.4093	3.1439	1.626E-07	6.97E+02
$3d^41$	$-3d^3(4P)4p$	$^1S^e$	$^5P^\circ$	1	5	3	4	4.4093	3.0195	8.343E-08	4.31E+02
$3d^41$	$-3d^3(4P)4p$	$^1S^e$	$^5D^\circ$	1	5	3	5	4.4093	3.0058	1.509E-09	7.96E+00
$3d^41$	$-3d^3(4P)4p$	$^1S^e$	$^3P^\circ$	1	5	3	6	4.4093	2.9911	2.573E-07	1.39E+03
$3d^41$	$-3d^3(2P)4p$	$^1S^e$	$^3P^\circ$	1	5	3	7	4.4093	2.9439	1.238E-05	7.12E+04
$3d^41$	$-3d^3(2D2)4p$	$^1S^e$	$^1P^\circ$	1	5	3	8	4.4093	2.9073	2.067E-05	1.25E+05
$3d^41$	$-3d^3(2D2)4p$	$^1S^e$	$^3D^\circ$	1	5	3	9	4.4093	2.8826	3.442E-04	2.15E+06
$3d^41$	$-3d^3(2P)4p$	$^1S^e$	$^3D^\circ$	1	5	3	10	4.4093	2.9274	1.868E-05	1.10E+05

Table 5. b) Fine-structure transitions, ordered in LS multiplets, compared with previous values

C_i	C_j	$S_iL_i\pi_i$	$S_jL_j\pi_j$	$2J_i+1$	I_i	$2J_j+1$	I_j	f_{ij}(present)	f_{ij}(others)
3d4	−3d3(4F)4p	5D0	5F1	1	1	3	1	0.2154	0.163[a]
3d4	−3d3(4F)4p	5D0	5F1	3	1	3	1	3.790E-04	
3d4	−3d3(4F)4p	5D0	5F1	3	1	5	3	0.00136	
3d4	−3d3(4F)4p	5D0	5F1	5	1	3	1	0.04617	0.0126[a]
3d4	−3d3(4F)4p	5D0	5F1	5	1	5	3	0.05967	0.0596[a]
3d4	−3d3(4F)4p	5D0	5F1	5	1	7	3	0.01462	0.0138[a]
3d4	−3d3(4F)4p	5D0	5F1	7	1	5	3	0.006895	0.0274[a]
3d4	−3d3(4F)4p	5D0	5F1	7	1	7	3	0.05889	0.0544[a]
3d4	−3d3(4F)4p	5D0	5F1	9	1	7	3	0.001966	0.00756[a]
3d4	−3d3(4F)4p	5D0	5F1	7	1	9	3	0.03262	0.0414[a]
3d4	−3d3(4F)4p	5D0	5F1	9	1	9	3	0.05139	0.03[a]
3d4	−3d3(4F)4p	5D0	5F1	9	1	11	2	0.07548	0.0686[a]
3d4	−3d3(4F)4p	5D0	5F1	25		35		0.107	0.0804[b],0.0915[c]
3d4	−3d3(4F)4p	5D0	5D1	1	1	3	2	0.00551	0.041[a]
3d4	−3d3(4F)4p	5D0	5D1	3	1	1	1	0.06255	0.0607[a]
3d4	−3d3(4F)4p	5D0	5D1	3	1	3	2	0.03888	0.0343[a]
3d4	−3d3(4F)4p	5D0	5D1	3	1	5	2	0.1360	0.1257[a]
3d4	−3d3(4F)4p	5D0	5D1	5	1	3	2	0.01704	0.0532[a]
3d4	−3d3(4F)4p	5D0	5D1	5	1	5	2	0.01372	0.0092[a]
3d4	−3d3(4F)4p	5D0	5D1	5	1	7	2	0.1087	0.1006[a]
3d4	−3d3(4F)4p	5D0	5D1	7	1	5	2	0.04155	0.0247[a]
3d4	−3d3(4F)4p	5D0	5D1	7	1	7	2	0.04936	0.0517[a]
3d4	−3d3(4F)4p	5D0	5D1	9	1	7	2	0.02644	0.0222[a]
3d4	−3d3(4F)4p	5D0	5D1	7	1	9	2	0.07311	0.0588[a]
3d4	−3d3(4F)4p	5D0	5D1	9	1	9	2	0.1168	0.130[a]
3d4	−3d3(4F)4p	5D0	5D1	25		25		0.1541	0.1708[b],0.192[c]
3d4	−3d3(4P)4p	5D0	5P1	1	1	3	4	0.08420	0.076[a]
3d4	−3d3(4P)4p	5D0	5P1	3	1	3	4	0.06281	0.057[a]
3d4	−3d3(4P)4p	5D0	5P1	3	1	5	6	0.02114	0.019[a]
3d4	−3d3(4P)4p	5D0	5P1	5	1	3	4	0.02926	0.0266[a]
3d4	−3d3(4P)4p	5D0	5P1	5	1	5	6	0.04831	0.0442[a]
3d4	−3d3(4P)4p	5D0	5P1	5	1	7	7	0.00622	0.0054[a]
3d4	−3d3(4P)4p	5D0	5P1	7	1	5	6	0.05555	0.0499[a]
3d4	−3d3(4P)4p	5D0	5P1	7	1	7	7	0.03105	0.0264[a]
3d4	−3d3(4P)4p	5D0	5P1	9	1	7	7	0.08782	0.0758[a]
3d4	−3d3(4P)4p	5D0	5P1	25		15		0.0861	0.076[b],0.0893[c]
3d4	−3d3(4P)4p	5D0	5D1	1	1	3	5	4.401E-03	
3d4	−3d3(4P)4p	5D0	5D1	3	1	1	2	4.902E-04	
3d4	−3d3(4P)4p	5D0	5D1	3	1	3	5	7.201E-04	
3d4	−3d3(4P)4p	5D0	5D1	3	1	5	7	2.402E-03	
3d4	−3d3(4P)4p	5D0	5D1	5	1	3	5	1.502E-03	
3d4	−3d3(4P)4p	5D0	5D1	5	1	5	7	2.248E-03	
3d4	−3d3(4P)4p	5D0	5D1	5	1	7	8	1.474E-03	
3d4	−3d3(4P)4p	5D0	5D1	7	1	5	7	2.675E-03	
3d4	−3d3(4P)4p	5D0	5D1	7	1	7	8	1.048E-03	
3d4	−3d3(4P)4p	5D0	5D1	9	1	7	8	2.846E-06	
3d4	−3d3(4P)4p	5D0	5D1	7	1	9	7	1.408E-03	
3d4	−3d3(4P)4p	5D0	5D1	9	1	9	7	4.558E-03	
3d4	−3d3(4P)4p	5D0	5D1	25		25		0.0047	0.00436[b],0.00564[c]
3d4 2	−3d3(4F)4p	3P0	3D1	1	2	3	3	6.702E-02	0.061[a]
3d4 2	−3d3(4F)4p	3P0	3D1	3	2	3	3	1.585E-02	0.0147[a]
3d4 2	−3d3(4F)4p	3P0	3D1	3	2	5	4	6.279E-02	0.057[a]
3d4 2	−3d3(4F)4p	3P0	3D1	5	2	3	3	6.685E-04	
3d4 2	−3d3(4F)4p	3P0	3D1	5	2	5	4	1.144E-02	0.011[a]
3d4 2	−3d3(4F)4p	3P0	3D1	5	2	7	4	7.753E-02	0.0756[a]
3d4 2	−3d3(4F)4p	3P0	3D1	9		15		0.0833	0.0973[b],0.106[c]
3d4 2	−3d3(4P)4p	3P0	3P1	1	2	3	6	1.907E-02	
3d4 2	−3d3(4P)4p	3P0	3P1	3	2	1	3	3.593E-03	
3d4 2	−3d3(4P)4p	3P0	3P1	3	2	3	6	3.409E-03	
3d4 2	−3d3(4P)4p	3P0	3P1	3	2	5	8	3.037E-03	
3d4 2	−3d3(4P)4p	3P0	3P1	5	2	3	6	3.742E-03	
3d4 2	−3d3(4P)4p	3P0	3P1	5	2	5	8	2.134E-03	
3d4 2	−3d3(4P)4p	3P0	3P1	9		9		0.0087	0.00542[b],0.0127[c]
3d4 2	−3d3(2P)4p	3P0	3S1	1	2	3	11	2.193E-03	
3d4 2	−3d3(2P)4p	3P0	3S1	3	2	3	11	5.853E-03	
3d4 2	−3d3(2P)4p	3P0	3S1	5	2	3	11	3.582E-04	
3d4 2	−3d3(2P)4p	3P0	3S1	9		3		0.00239	0.00142[b],0.056[c]

[a]Fawcett (1989), [b]Butler, [c]Bautista (1996).

Table 6. Comparison of A-values for forbidden transitions, $A_{fi}^{\rm cal}$, among $3d^4$ fine-structure levels with those, $A_{fi}^{\rm G}$, by Garstang (1957)

Transition		$\lambda_{\rm vac}$	$E_i(\rm cm^{-1})$	$E_f(\rm cm^{-1})$	$A_{fi}^{\rm G}(\rm s^{-1})$	$A_{fi}^{\rm cal}(\rm s^{-1})$
$^5D_1$	$^3P2_0$	4181.8	142.1	24055.4	1.30E+00	1.39E+00
$^5D_0$	$^3P2_1$	4004.3	0.0	24972.9	1.30E-01	1.23E-01
$^5D_2$	$^3P2_1$	4072.4	417.3	24972.9	1.10E+00	1.07E+00
$^5D_1$	$^3P2_2$	3798.5	142.1	26468.3	3.60E-02	3.54E-02
$^5D_3$	$^3P2_2$	3896.3	803.1	26468.3	7.10E-01	7.08E-01
$^5D_4$	$^3H_4$	4228.4	1282.8	24932.5	1.10E-03	4.34E-03
$^5D_1$	$^3F2_2$	3756.8	142.1	26760.7	1.00E-01	1.04E-01
$^5D_2$	$^3F2_2$	3796.0	417.3	26760.7	2.00E-01	2.01E-01
$^5D_3$	$^3F2_2$	3852.4	803.1	26760.7	4.70E-02	5.25E-02
$^5D_2$	$^3F2_3$	3784.3	417.3	26842.3	1.60E-01	1.78E-01
$^5D_3$	$^3F2_3$	3840.4	803.1	26842.3	4.00E-01	4.66E-01
$^5D_4$	$^3F2_3$	3912.4	1282.8	26842.3	6.60E-02	6.43E-02
$^5D_3$	$^3F2_4$	3821.0	803.1	26974.0	1.60E-01	1.66E-01
$^5D_4$	$^3F2_4$	3892.4	1282.8	26974.0	7.40E-01	7.92E-01
$^5D_2$	$^3G_3$	3401.4	417.3	29817.1	7.00E-03	6.76E-03
$^5D_3$	$^3G_3$	3446.6	803.1	29817.1	1.70E-02	1.62E-02
$^5D_4$	$^3G_3$	3504.6	1282.8	29817.1	2.60E-03	2.32E-03
$^5D_3$	$^3G_4$	3407.9	803.1	30147.0	7.80E-03	7.20E-03
$^5D_4$	$^3G_4$	3464.5	1282.8	30147.0	3.20E-02	2.58E-02
$^5D_2$	$^3D_3$	2761.5	417.3	36630.1	9.70E-02	9.76E-02
$^5D_3$	$^3D_3$	2791.2	803.1	36630.1	8.90E-02	9.15E-02
$^5D_4$	$^3D_3$	2829.1	1282.8	36630.1	3.70E-01	3.80E-01
$^5D_1$	$^3D_2$	2731.0	142.1	36758.5	2.00E-01	1.96E-01
$^5D_2$	$^3D_2$	2751.7	417.3	36758.5	1.80E-01	1.60E-01
$^5D_3$	$^3D_2$	2781.2	803.1	36758.5	1.10E-01	1.05E-01
$^5D_0$	$^3D_1$	2708.2	0.0	36925.4	2.20E-01	2.37E-01
$^5D_1$	$^3D_1$	2718.6	142.1	36925.4	1.90E-01	2.11E-01
$^5D_2$	$^3D_1$	2739.1	417.3	36925.4	1.90E-03	2.73E-03
$^3H_4$	$^3G_3$	20472.5	24932.5	29817.1	3.60E-02	3.98E-02
$^3H_4$	$^3G_4$	19177.3	24932.5	30147.0	3.30E-02	3.33E-02
$^3H_4$	$^3G_5$	18189.8	24932.5	30430.1	1.20E-03	8.77E-04
$^3H_5$	$^3G_5$	19215.2	25225.9	30430.1	4.10E-02	4.40E-02
$^3H_6$	$^3G_5$	20401.5	25528.5	30430.1	4.10E-02	4.39E-02
$^3H_5$	$^1I_6$	8139.5	25225.9	37511.7	1.10E-01	1.16E-01
$^3H_6$	$^1I_6$	8345.0	25528.5	37511.7	1.40E-01	1.52E-01
$^3F2_2$	$^3G_3$	32718.2	26760.7	29817.1	3.00E-02	3.03E-02
$^3F2_3$	$^3G_3$	33615.7	26842.3	29817.1	3.70E-02	3.76E-02
$^3F2_4$	$^3G_4$	31515.9	26974.0	30147.0	2.70E-02	2.80E-02
$^3F2_4$	$^3G_5$	28934.3	26974.0	30430.1	3.70E-02	3.74E-02
$^3F2_3$	$^3D_3$	10216.8	26842.3	36630.1	6.40E-03	5.97E-03
$^3F2_4$	$^3D_3$	10356.1	26974.0	36630.1	6.90E-03	6.37E-03
$^3F2_2$	$^3D_2$	10002.2	26760.7	36758.5	1.70E-02	1.44E-02
$^3F2_3$	$^3D_2$	10084.5	26842.3	36758.5	1.60E-03	1.21E-03
$^3F2_2$	$^3D_1$	9838.0	26760.7	36925.4	1.40E-02	1.36E-02
$^3F2_2$	$^1D2_2$	5120.2	26760.7	46291.2	2.10E-01	2.28E-01
$^3F2_3$	$^1D2_2$	5141.7	26842.3	46291.2	4.20E-01	4.48E-01
$^3G_3$	$^1F_3$	4363.8	29817.1	52732.7	1.20E-01	1.23E-01
$^3G_4$	$^1F_3$	4427.6	30147.0	52732.7	1.70E-01	1.70E-01
$^3D_3$	$^1D2_2$	10350.8	36630.1	46291.2	9.00E-02	1.08E-01
$^3D_2$	$^1D2_2$	10490.2	36758.5	46291.2	1.70E-02	2.00E-02
$^3D_1$	$^1D2_2$	10677.1	36925.4	46291.2	8.00E-02	9.60E-02
$^3D_3$	$^1F_3$	6210.2	36630.1	52732.7	1.50E-01	1.65E-01
$^3D_2$	$^1F_3$	6260.1	36758.5	52732.7	7.00E-02	7.41E-02

All data tables will be electronically available from the CDS archives, and via ftp from the first author at: nahar@astronomy.ohio-state.edu.

Acknowledgements. We would like to thank Dr. Werner Eissner for helpful comments and general assistance with the BPRM codes. This work was partially supported by U.S. National Science Foundation (AST-9870089) and the NASA (NAG5 7903). The computational work was carried out on the Cray T94 at the Ohio Supercomputer Center in Columbus, Ohio. The collaboration between Columbus and Meudon benefitted from a visit to the DAEC by AKP, with support from the Université Paris 7.

References

Bautista M.A., 1996, A&AS 119, 105

Berrington K.A., Burke P.G., Butler K., et al., 1987, J. Phys. B 20, 6379

Berrington K.A., Eissner W.B., Norrington P.H., 1995, Comput. Phys. Commun. 92, 290

Berrington K.A., Pelan J., Quigley L., 1998, Phys. Scr. 57, 549

Table 7. Forbidden transitions in Fe V

C_i	C_j	$S_iL_i\Pi_i$	$S_jL_j\Pi_j$	J_i	J_j	$\lambda_{\rm vac}$	$E_i(\rm cm^{-1})$	$E_j(\rm cm^{-1})$	$A^{\rm M1}_{ji}(\rm s^{-1})$	$A^{\rm E2}_{ji}(\rm s^{-1})$
$3d^4$	$3d^4$	^{5}D	^{5}D	0	1	703729.8	0.0	142.1	1.55E-04	0.00E+00
$3d^4$	$3d^4$	^{5}D	^{5}D	0	2	239635.8	0.0	417.3	0.00E+00	1.17E-10
$3d^4$	$3d^4$	^{5}D	^{5}D	1	2	363372.1	142.1	417.3	1.18E-03	1.10E-11
$3d^4$	$3d^4$	^{5}D	^{5}D	1	3	151285.9	142.1	803.1	0.00E+00	1.00E-09
$3d^4$	$3d^4$	^{5}D	^{5}D	2	3	259201.7	417.3	803.1	2.65E-03	1.29E-10
$3d^4$	$3d^4$	^{5}D	^{5}D	2	4	115540.2	417.3	1282.8	0.00E+00	1.84E-09
$3d^4$	$3d^4$	^{5}D	^{5}D	3	4	208463.6	803.1	1282.8	2.98E-03	4.19E-10
$3d^4$	$3d^4$	^{5}D	^{3}P2	2	0	4230.5	417.3	24055.4	0.00E+00	4.75E-04
$3d^4$	$3d^4$	^{5}D	^{3}P2	1	1	4027.3	142.1	24972.9	8.72E-05	2.01E-04
$3d^4$	$3d^4$	^{5}D	^{3}P2	3	1	4137.4	803.1	24972.9	0.00E+00	7.02E-05
$3d^4$	$3d^4$	^{5}D	^{3}P2	0	2	3778.1	0.0	26468.3	0.00E+00	6.83E-05
$3d^4$	$3d^4$	^{5}D	^{3}P2	2	2	3838.6	417.3	26468.3	3.52E-05	2.00E-05
$3d^4$	$3d^4$	^{5}D	^{3}P2	4	2	3970.5	1282.8	26468.3	0.00E+00	2.04E-05
$3d^4$	$3d^4$	^{5}D	^{3}H	2	4	4079.1	417.3	24932.5	0.00E+00	1.44E-07
$3d^4$	$3d^4$	^{5}D	^{3}H	3	4	4144.3	803.1	24932.5	8.32E-04	1.15E-09
$3d^4$	$3d^4$	^{5}D	^{3}H	3	5	4094.5	803.1	25225.9	0.00E+00	2.15E-06
$3d^4$	$3d^4$	^{5}D	^{3}H	4	5	4176.6	1282.8	25225.9	1.25E-05	1.09E-07
$3d^4$	$3d^4$	^{5}D	^{3}H	4	6	4124.4	1282.8	25528.5	0.00E+00	1.67E-05
$3d^4$	$3d^4$	^{5}D	^{3}F2	0	2	3736.8	0.0	26760.7	0.00E+00	3.67E-05
$3d^4$	$3d^4$	^{5}D	^{3}F2	4	2	3925.0	1282.8	26760.7	0.00E+00	2.54E-06
$3d^4$	$3d^4$	^{5}D	^{3}F2	1	3	3745.3	142.1	26842.3	0.00E+00	1.28E-05
$3d^4$	$3d^4$	^{5}D	^{3}F2	2	4	3765.5	417.3	26974.0	0.00E+00	1.14E-06
$3d^4$	$3d^4$	^{5}D	^{3}G	1	3	3369.8	142.1	29817.1	0.00E+00	5.37E-05
$3d^4$	$3d^4$	^{5}D	^{3}G	2	4	3363.6	417.3	30147.0	0.00E+00	8.67E-05
$3d^4$	$3d^4$	^{5}D	^{3}G	3	5	3375.3	803.1	30430.1	0.00E+00	8.86E-05
$3d^4$	$3d^4$	^{5}D	^{3}G	4	5	3430.8	1282.8	30430.1	5.93E-04	2.13E-04
$3d^4$	$3d^3$(4F)	^{5}D	^{5}F	0	1	536.4	0.0	186433.6	6.97E-05	0.00E+00
$3d^4$	$3d^3$(4F)	^{5}D	^{5}F	1	1	536.8	142.1	186433.6	1.59E-04	1.54E+04
$3d^4$	$3d^3$(4F)	^{5}D	^{5}F	2	1	537.6	417.3	186433.6	6.48E-05	1.09E+04
$3d^4$	$3d^3$(4F)	^{5}D	^{5}F	3	1	538.7	803.1	186433.6	0.00E+00	1.09E+03
$3d^4$	$3d^3$(4F)	^{5}D	^{5}F	0	2	535.5	0.0	186725.5	0.00E+00	7.79E+03
$3d^4$	$3d^3$(4F)	^{5}D	^{5}F	1	2	536.0	142.1	186725.5	1.77E-05	1.90E-04
$3d^4$	$3d^3$(4F)	^{5}D	^{5}F	2	2	536.7	417.3	186725.5	1.26E-04	1.26E+04
$3d^4$	$3d^3$(4F)	^{5}D	^{5}F	3	2	537.9	803.1	186725.5	5.30E-05	6.83E+03
$3d^4$	$3d^3$(4F)	^{5}D	^{5}F	4	2	539.3	1282.8	186725.5	0.00E+00	3.51E+02
$3d^4$	$3d^3$(4F)	^{5}D	^{5}F	1	3	534.7	142.1	187157.5	0.00E+00	1.01E+04
$3d^4$	$3d^3$(4F)	^{5}D	^{5}F	2	3	535.5	417.3	187157.5	4.29E-07	1.19E+03
$3d^4$	$3d^3$(4F)	^{5}D	^{5}F	3	3	536.6	803.1	187157.5	8.40E-05	1.35E+04
$3d^4$	$3d^3$(4F)	^{5}D	^{5}F	4	3	538.0	1282.8	187157.5	2.36E-05	2.94E+03
$3d^4$	$3d^3$(4F)	^{5}D	^{5}F	2	4	533.9	417.3	187719.0	0.00E+00	1.01E+04
$3d^4$	$3d^3$(4F)	^{5}D	^{5}F	3	4	535.0	803.1	187719.0	3.95E-05	6.97E+03
$3d^4$	$3d^3$(4F)	^{5}D	^{5}F	4	4	536.4	1282.8	187719.0	4.06E-05	1.09E+04
$3d^4$	$3d^3$(4F)	^{5}D	^{5}F	3	5	533.1	803.1	188395.3	0.00E+00	7.09E+03
$3d^4$	$3d^3$(4F)	^{5}D	^{5}F	4	5	534.4	1282.8	188395.3	1.56E-04	2.10E+04
$3d^4$	$3d^4$	^{3}P2	^{3}P2	0	1	108991.8	24055.4	24972.9	1.38E-02	0.00E+00
$3d^4$	$3d^4$	^{3}P2	^{3}P2	0	2	41443.9	24055.4	26468.3	0.00E+00	8.70E-09
$3d^4$	$3d^4$	^{3}P2	^{3}P2	1	2	66871.7	24972.9	26468.3	4.52E-02	1.97E-09
$3d^4$	$3d^4$	^{3}P2	^{3}F2	0	2	36964.5	24055.4	26760.7	0.00E+00	3.47E-07
$3d^4$	$3d^4$	^{3}P2	^{3}F2	1	2	55934.7	24972.9	26760.7	2.22E-05	4.87E-08
$3d^4$	$3d^4$	^{3}P2	^{3}F2	2	2	341997.3	26468.3	26760.7	7.92E-07	1.19E-12
$3d^4$	$3d^4$	^{3}P2	^{3}F2	1	3	53493.1	24972.9	26842.3	0.00E+00	6.78E-08
$3d^4$	$3d^4$	^{3}P2	^{3}F2	2	3	267379.7	26468.3	26842.3	3.55E-07	1.48E-11
$3d^4$	$3d^4$	^{3}P2	^{3}F2	2	4	197745.7	26468.3	26974.0	0.00E+00	1.38E-10
$3d^4$	$3d^4$	^{3}P2	^{3}G	1	3	20643.2	24972.9	29817.1	0.00E+00	7.16E-08
$3d^4$	$3d^4$	^{3}P2	^{3}G	2	3	29861.4	26468.3	29817.1	1.16E-05	1.36E-08
$3d^4$	$3d^4$	^{3}P2	^{3}G	2	4	27183.5	26468.3	30147.0	0.00E+00	1.00E-08
$3d^4$	$3d^3$(4F)	^{3}P2	^{5}F	0	1	615.8	24055.4	186433.6	6.41E-08	0.00E+00
$3d^4$	$3d^3$(4F)	^{3}P2	^{5}F	1	1	619.3	24972.9	186433.6	6.00E-07	1.12E+00
$3d^4$	$3d^3$(4F)	^{3}P2	^{5}F	2	1	625.1	26468.3	186433.6	9.64E-08	3.48E-01
$3d^4$	$3d^3$(4F)	^{3}P2	^{5}F	0	2	614.7	24055.4	186725.5	0.00E+00	2.06E-01

Table 7. continued

C_i	C_j	$S_iL_i\Pi_i$	$S_jL_j\Pi_j$	J_i	J_j	$\lambda_{\rm vac}$	$E_i(\rm cm^{-1})$	$E_j(\rm cm^{-1})$	$A_{ji}^{\rm M1}(\rm s^{-1})$	$A_{ji}^{\rm E2}(\rm s^{-1})$
$3d^4$	$3d^3(4F)$	^{3}P2	^{5}F	1	2	618.2	24972.9	186725.5	1.68E-07	1.63E-01
$3d^4$	$3d^3(4F)$	^{3}P2	^{5}F	2	2	624.0	26468.3	186725.5	3.12E-07	6.09E-01
$3d^4$	$3d^3(4F)$	^{3}P2	^{5}F	1	3	616.6	24972.9	187157.5	0.00E+00	4.94E-02
$3d^4$	$3d^3(4F)$	^{3}P2	^{5}F	2	3	622.3	26468.3	187157.5	6.44E-07	3.56E-01
$3d^4$	$3d^3(4F)$	^{3}P2	^{5}F	2	4	620.2	26468.3	187719.0	0.00E+00	5.32E-03
$3d^4$	$3d^4$	^{3}H	^{3}P2	4	2	65112.6	24932.5	26468.3	0.00E+00	6.81E-10
$3d^4$	$3d^4$	^{3}H	^{3}H	4	5	340831.6	24932.5	25225.9	6.60E-04	1.09E-13
$3d^4$	$3d^4$	^{3}H	^{3}H	4	6	167785.2	24932.5	25528.5	0.00E+00	2.54E-12
$3d^4$	$3d^4$	^{3}H	^{3}H	5	6	330469.3	25225.9	25528.5	6.12E-04	6.75E-15
$3d^4$	$3d^4$	^{3}H	^{3}F2	4	2	54698.6	24932.5	26760.7	0.00E+00	9.98E-08
$3d^4$	$3d^4$	^{3}H	^{3}F2	4	3	52361.5	24932.5	26842.3	1.55E-03	1.85E-08
$3d^4$	$3d^4$	^{3}H	^{3}F2	5	3	61865.9	25225.9	26842.3	0.00E+00	6.77E-08
$3d^4$	$3d^4$	^{3}H	^{3}F2	4	4	48983.6	24932.5	26974.0	6.05E-03	1.10E-10
$3d^4$	$3d^4$	^{3}H	^{3}F2	5	4	57205.0	25225.9	26974.0	9.40E-04	1.17E-08
$3d^4$	$3d^4$	^{3}H	^{3}F2	6	4	69180.2	25528.5	26974.0	0.00E+00	3.72E-08
$3d^4$	$3d^4$	^{3}H	^{3}G	5	3	21780.8	25225.9	29817.1	0.00E+00	4.24E-06
$3d^4$	$3d^4$	^{3}H	^{3}G	5	4	20320.7	25225.9	30147.0	4.59E-04	9.52E-05
$3d^4$	$3d^4$	^{3}H	^{3}G	6	4	21652.1	25528.5	30147.0	0.00E+00	3.21E-06
$3d^4$	$3d^3(4F)$	^{3}H	^{5}F	4	2	618.1	24932.5	186725.5	0.00E+00	1.66E+01
$3d^4$	$3d^3(4F)$	^{3}H	^{5}F	4	3	616.4	24932.5	187157.5	1.72E-06	3.91E+00
$3d^4$	$3d^3(4F)$	^{3}H	^{5}F	5	3	617.5	25225.9	187157.5	0.00E+00	2.08E+01
$3d^4$	$3d^3(4F)$	^{3}H	^{5}F	4	4	614.3	24932.5	187719.0	2.68E-06	2.75E-01
$3d^4$	$3d^3(4F)$	^{3}H	^{5}F	5	4	615.4	25225.9	187719.0	5.44E-07	6.70E+00
$3d^4$	$3d^3(4F)$	^{3}H	^{5}F	6	4	616.6	25528.5	187719.0	0.00E+00	1.47E+01
$3d^4$	$3d^3(4F)$	^{3}H	^{5}F	4	5	611.8	24932.5	188395.3	1.06E-07	3.46E-03
$3d^4$	$3d^3(4F)$	^{3}H	^{5}F	5	5	612.9	25225.9	188395.3	3.70E-06	2.25E-01
$3d^4$	$3d^3(4F)$	^{3}H	^{5}F	6	5	614.0	25528.5	188395.3	3.61E-07	8.33E+00
$3d^4$	$3d^4$	^{3}F2	^{3}F2	2	3	1225490.2	26760.7	26842.3	1.34E-05	4.26E-15
$3d^4$	$3d^4$	^{3}F2	^{3}F2	2	4	468823.3	26760.7	26974.0	0.00E+00	5.33E-15
$3d^4$	$3d^4$	^{3}F2	^{3}F2	3	4	759301.4	26842.3	26974.0	4.60E-05	2.91E-14
$3d^4$	$3d^4$	^{3}F2	^{3}G	4	3	35172.9	26974.0	29817.1	1.89E-04	1.37E-07
$3d^4$	$3d^4$	^{3}F2	^{3}G	2	4	29530.8	26760.7	30147.0	0.00E+00	1.13E-07
$3d^4$	$3d^4$	^{3}F2	^{3}G	3	4	30259.9	26842.3	30147.0	7.94E-04	1.22E-06
$3d^4$	$3d^4$	^{3}F2	^{3}G	3	5	27872.2	26842.3	30430.1	0.00E+00	8.99E-08
$3d^4$	$3d^4$	^{3}G	^{3}G	3	4	303122.2	29817.1	30147.0	9.18E-04	5.80E-13
$3d^4$	$3d^4$	^{3}G	^{3}G	3	5	163132.1	29817.1	30430.1	0.00E+00	3.11E-12
$3d^4$	$3d^4$	^{3}G	^{3}G	4	5	353232.1	30147.0	30430.1	4.69E-04	5.41E-13

Biémont E., Delahaye F., Zeippen C.J., 1994, J. Phys. B 27, 5841

Burke P.G., Hibbert A., Robb W.D., 1971, J. Phys. B 4, 153

Butler K. (unpublished); data are available through the OP database, TOPbase, Cunto W., Mendoza C., Ochsenbein F., Zeippen C.J. (eds.), 1993, A&A 275, L5

Chen G.X., Pradhan A.K., 1999, J. Phys. B 32, 1809

Eissner W., Jones M., Nussbaumer H., 1974, Comput. Phys. Commun. 8, 270

Eissner W., Jones M., Nussbaumer H., Comput. Phys. Commun. 8, 270 (1974); Eissner W., 1991, J. Phys. IV (Paris) C1, 3

Fawcett B.C., 1989, At. Data Nucl. Data Tab. 41, 181

Garstang R.H., 1957, MNRAS 117, 393

Hui-Bon-Hoa A., Alecian G., 1998, A&A 332, 224

Hummer D.G., Berrington K.A., Eissner W., et al., 1993, A&A 279, 298

Nahar S.N., 1995, A&A 293, 967

Nahar S.N., 1999, At. Data Nucl. Data Tab. 72, 129

Nahar S.N., Pradhan A.K., 1996, A&AS 119, 509

Nahar S.N., Pradhan A.K., 1999, A&AS 135, 347

Nahar S.N., Pradhan A.K., 2000, Phys. Scr. 61, xxxx

Quinet P., Hansen, 1995, J. Phys. B 28, L213

Ramírez J.M., Nahar S.N., Mendoza C., Berrington K.A., 2000 (in preparation)

Nussbaumer H., Storey P.J., 1978, A&A 64, 139

Sawey P.M.J., Berrington K.A., 1992, J. Phys. B 25, 1451

Scott N.S., Burke P.G., 1980, J. Phys. B 12, 4299

Scott N.S., Taylor K.T., 1982, Comput. Phys. Commun. 25, 347

Seaton M.J., 1987, J. Phys. B 20, 6363

Seaton M.J., 1997, MNRAS 289, 700

Seaton M.J., 1999, MNRAS 307, 1008

Seaton M.J., Yu Y., Mihalas D., Pradhan A.K., 1994, MNRAS 266, 805

Sugar J., Corliss C., 1985, J. Phys. Chem. Ref. Data 14, Suppl. 2

The Opacity Project Team, Vol. 1, 1995. Institute of Physics Publishing, Bristol & Philadelphia, ISBN 0 7503 0288 7

The Opacity Project Team, Vol. 2, 1996. Institute of Physics Publishing, Bristol & Philadelphia, ISBN 0 7503 0174 0

Zeippen C.J., Seaton M.J., Morton D.C., 1977, MNRAS 181, 527